Supplementary Information for

Deciphering the Shape Selective Conformational Equilibrium of *E*- and *Z*-Locked Azobenzene-Tetraethyl Ammonium Ion in Regulating Photo-switchable K^+-ion Channel Blocking

Rinsha Cholasseri[a] and Susmita De*[b]

*Corresponding Author

[a]Theoretical and Computational Chemistry Laboratory, Department of Chemistry, National Institute of Technology Calicut, Kozhikode, Kerala, India - 673 601.

[b]Department of Chemistry, University of Calicut, Calicut University P. O., Malappuram, Kerala, India - 673 635. E-mail: susmita@uoc.ac.in

The Supporting Information contains,

- Supplementary Scheme Legends.
- Supplementary Figure Legends.
- Supplementary Table Legends.
- Supplementary Movie Legends
- Supplementary Scheme S1.
- Supplementary Figures S1-S35.
- Supplementary Table S1.
- Supplementary Movies S1-S5

Supplementary Scheme Legends

Scheme S1. Schematic representation of KcsA-LAB-TEA starting conformations used for the simulation without K^+-ion. The open KcsA (PDB ID: 3F5W) showing only two diagonally opposite subunits, and is represented as a new cartoon. The TEA and amino-acids represented by

ball and stick model (red = threonine (THR-75 and THR-107), purple = glycine (GLY-99), blue = isoleucine (ILE-100), green = phenylalanine (PHE-103), ochre = valine (VAL-106 and VAL-115), grey = leucine (LEU-110)). The azo-nitrogens and TEA nitrogen are shown as blue in colour. The purple ball represents the potassium ion. And d represents the distance between the center of C_α of THR-75 and nitrogen of TEA.

Supplementary Figure Legends

Figure S1. Starting structures resulted after equilibration for the molecular dynamics simulation of *Z*1 (*Z*1a-*Z*lh), *Z*2 (*Z*2a-*Z*2h), *E*1 (*E*1a-*E*lh) and *E*2-isomers (*E*2a-*E*2h) of LAB-TEA (stick model) with KcsA-K^+-ion channel (new cartoon representation in grey colour) with one K^+-ion (purple ball). LAB-TEA is in the cytoplasmic region. The amino-acid residue THR-107 (red) shown in ball and stick model. Note that we have not studied the dynamics of $Z \leftrightarrow E$ photo-isomerization inside the potassium ion channel directly. All the structures were subjected to 100 ns simulation except *Z*1a, *Z*2a, *E*1a, and *E*2a (400 ns).

Figure S2. Dihedral angle plot (Time (ns) vs. Dihedral angle (degree)) for *Z*-LAB-TEA when placed in the cytoplasmic region during simulation with one K^+-ion. The red line represents the average dihedral angle in degrees.

Figure S3. Dihedral angle plot (Time (ns) vs. Dihedral angle (degree)) for *E*-LAB-TEA when placed in the cytoplasmic region during simulation with one K^+-ion. The red line represents the average dihedral angle in degrees.

Figure S4. Distance plot (Time (ns) vs. Distance (Å)) showing variation in the K^+-$C_{\alpha THR\text{-}75}$ distances during the simulations started with *Z*1 with one K^+-ion. The red line represents the average value in Angstrom.

Figure S5. Distance plot (Time (ns) vs. Distance (Å)) showing variation in the K^+-$C_{\alpha THR\text{-}75}$ distances during the simulations started with *Z*2 with one K^+-ion. The red line represents the average value in Angstrom.

Figure S6. Distance plot (Time (ns) vs. Distance (Å)) showing variation in the K^+-$C_{\alpha THR\text{-}75}$ distances during the simulations started with *E*1 with one K^+-ion. The red line represents the average value in Angstrom.

Figure S7. Distance plot (Time (ns) vs. Distance (Å)) showing variation in the K^+-$C_{\alpha THR\text{-}75}$ distances during the simulations started with *E*2 with one K^+-ion. The red line represents the average value in Angstrom.

Figure S8. Distance plot (Time (ns) vs. Distance (Å)) showing variation in the $_{TEA}N$-$C_{\alpha THR\text{-}75}$ distances during the simulations started with *Z*1 with one K^+-ion. The red line represents the average value in Angstrom. The starting position and the preferable position of LAB-TEA during the simulation are shown in left and right insets, respectively.

Figure S9. Distance plot (Time (ns) vs. Distance (Å)) showing variation in the $_{TEA}N$-$C_{\alpha THR\text{-}75}$ distances during the simulations started with *Z*2 with one K^+-ion. The red line represents the average value in Angstrom. The starting position and the preferable position of LAB-TEA during the simulation shown in left and right insets, respectively.

Figure S10. Distance plot (Time (ns) vs. Distance (Å)) showing variation in the $_{TEA}N\text{-}C_{\alpha THR\text{-}75}$ distances during the simulations started with *E*1 with one K^+-ion. The red line represents the average value in Angstrom. The starting position and the preferable position of LAB-TEA during the simulation are shown in left and right insets, respectively.

Figure S11. Distance plot (Time (ns) vs. Distance (Å)) showing variation in the $_{TEA}N\text{-}C_{\alpha THR\text{-}75}$ distances during the simulations started with *E*2 with one K^+-ion. The red line represents the average value in Angstrom. The starting position and the preferable position of LAB-TEA during the simulation are shown in left and right insets, respectively.

Figure S12. Summary of hierarchical average-linkage clustering performed on trajectories of *Z*-LAB-TEA with one K^+-ion (purple ball) showing binding of *Z*-isomer into the channel cavity, when LAB-TEA placed in the cytoplasmic region. *Z*1a and *Z*1h are the starting structures resulting in *Z*1 and *Z*2 binding conformations respectively. The average structure of each cluster is shown, indicating location of LAB-TEA relative to the ion channel. Cn (n = 0 − 4) indicates different clusters. Percentage occurrence of each cluster is given in parenthesis. Corresponding binding energy (B.E.) is given in kcal/mol. Protein is represented as new cartoon in the starting structure and as lines in the average structures. LAB-TEA is shown as a stick model.

Figure S13. Root-mean-square deviation plot (Time (ns) vs. RMSD (Å)) for *Z*-LAB-TEA with one K^+-ion resulting in the entry of *Z*-isomer to the channel cavity, when LAB-TEA placed in the cytoplasmic region. *Z*1a and *Z*1h are the starting structure for that particular trajectory resulting in *Z*1 and *Z*2 respectively. Black, red, and green graphs show RMSD of KcsA with *Z*-LAB-TEA, KcsA alone, and *Z*-LAB-TEA alone respectively.

Figure S14. Contact plot per residue for the most probable cluster trajectories (Cn with percentage > 10) of KcsA−*Z*-LAB-TEA with K^+-ion resulting in *Z*1 and *Z*2 conformations, when LAB-TEA placed in the cytoplasmic region. Binding energy in kcal/mol is given in parenthesis. The SF, CC, and CG represent selectivity filter, channel cavity, and channel gate residues respectively.

Figure S15. Interaction of *Z*2 conformation with individual channel residues in the most probable conformation (C0), of the trajectory resulting in *Z*-entry to the KcsA channel cavity, when simulation performed with one K^+-ion (purple ball model) inside the channel and *Z*-LAB-QA in the cytoplasmic region. The protein and *Z*2 represented as ribbon and stick (magenta) respectively, and the interacting residues THR-75 (red), ILE-100 (blue), PHE-103 (green), GLY- 104 (purple), and THR-107 (red) from extracellular to intracellular region in ball and stick model. The distances are given in Angstrom. Residue numbers are given in the upper left corner of each box.

Figure S16. Summary of hierarchical average-linkage clustering performed on trajectories of *E*-LAB-TEA with one K^+-ion (purple ball) showing entry of *E*-isomer into the channel cavity, when LAB-TEA placed in the cytoplasmic region, and resulting in *E*1 conformation. Structures *E*1a to *E*1h are the starting structure for that particular trajectory. The average structure of each cluster is shown, indicating location of LAB-TEA relative to the ion channel. Cn (n = 0 − 4) indicates different clusters. Percentage occurrence of each cluster is given in parenthesis. Corresponding binding energy (B.E.) is given in kcal/mol. Protein is represented as new cartoon in the starting structure and as lines in the average structures. LAB-TEA is shown as a stick model.

Figure S17. Summary of hierarchical average-linkage clustering performed on trajectories of *E*-LAB-TEA with one K^+-ion (purple ball) showing entry of *E*-isomer into the channel cavity, when LAB-TEA placed in the cytoplasmic region, resulting in *E*2 conformation. *E*1c to *E*2h are the starting structure for that particular trajectory. The average structure of each cluster is shown, indicating the location of LAB-TEA relative to the ion channel. Cn (n = 0 − 4) indicates different clusters. Percentage occurrence of each cluster is given in parenthesis. Corresponding binding energy (B.E.) is given in kcal/mol. Protein is represented as new cartoon in the starting structure and as lines in the average structures. LAB-TEA is shown as a stick model.

Figure S18. Root-mean-square deviation plot (Time (ns) vs. RMSD (Å)) for *E*-LAB-TEA with one K^+-ion resulting entry of *E*-isomer to the channel cavity, when LAB-TEA placed in the cytoplasmic region. *E*1a to *E*2h are the starting structure for that particular trajectory. Black, red, and green graphs show RMSD of KcsA with *E*-LAB-TEA, KcsA alone, and *E*-LAB-TEA alone respectively. The red line represents the average value in Angstrom.

Figure S19. Contact plot per residue for the most probable cluster trajectories (Cn with percentage > 10) of KcsA−*E*-LAB-TEA with K^+-ion resulting in *E*1 (*E*1a, *E*1b, *E*1d, *E*1f, *E*1g, and *E*1h) conformation, when LAB-TEA placed in the cytoplasmic region. Binding energy in kcal/mol is given in parenthesis. The SF, CC, and CG represent selectivity filter, channel cavity, and channel gate residues respectively.

Figure S20. Contact plot per residue for the most probable cluster trajectories (Cn with percentage > 10) of KcsA−*E*-LAB-TEA with K^+-ion resulting in *E*2 conformation, when LAB-TEA placed in the cytoplasmic region. Binding energy in kcal/mol is given in parenthesis. The SF, CC, and CG represent selectivity filter, channel cavity, and channel gate residues respectively.

Figure S21. Starting structures for the molecular dynamics simulation of *Z*- and *E*-isomers of LAB-TEA (stick model) with KcsA-K^+-ion channel (new cartoon representation in grey colour) in the absence of K^+-ion. The LAB-TEA is inside the channel. The amino-acid residue THR-107 (red) shown in ball and stick model.

Figure S22. Dihedral angle plot (Time (ns) vs. Dihedral angle (degree)) for *Z*-LAB-TEA when placed inside the channel during simulation without K^+-ion. *Z*1a to *Z*2e represent the starting structure for that particular trajectory. The red line represents the average dihedral angle in degrees.

Figure S23. Dihedral angle plot (Time (ns) vs. Dihedral angle (degree)) for *E*-LAB-TEA when placed inside the channel during simulation without K^+-ion. *E*1a to *E*2e represent the starting structure for that particular trajectory. The red line represents the average dihedral angle in degrees.

Figure S24. Summary of hierarchical average-linkage clustering performed on trajectories of *Z*-LAB-TEA without K^+-ion, when LAB-TEA placed inside the channel cavity. Z1a to *Z*1e are the starting structure for that particular trajectory. The average structure of each cluster is shown, indicating location of LAB-TEA relative to the ion channel. Cn (n = 0 − 4) indicates different clusters. Percentage occurrence of each cluster is given in parenthesis. Corresponding binding energy (B.E.) is given in kcal/mol. Protein is represented as new cartoon in the starting structure and as lines in the average structures. LAB-TEA is shown as a stick model. All the simulations retained the Z1 binding poses as that in the starting structure.

Figure S25. Contact plot per residue for the most probable cluster trajectories (Cn with percentage > 10) of KcsA−*Z*-LAB-QA without K^+-ion resulting in *Z*1 conformation, when LAB-TEA placed inside the channel cavity. Binding energy in kcal/mol is given in parenthesis. The SF, CC, and CG represent selectivity filter, channel cavity, and channel gate residues respectively.

Figure S26. Summary of hierarchical average-linkage clustering performed on trajectories of *Z*-LAB-TEA without K^+-ion, when LAB-TEA placed inside the channel cavity in *Z*2 conformation. *Z*2a to *Z*2e are the starting structure for that particular trajectory. The average structure of each cluster is shown, indicating location of LAB-TEA relative to the ion channel. Cn (n = 0 − 4) indicates different clusters. Percentage occurrence of each cluster is given in parenthesis. Corresponding binding energy (B.E.) is given in kcal/mol. Protein is represented as new cartoon in the starting structure and as lines in the average structures. LAB-TEA is shown as a stick model. All the simulations result in *Z*2 to *Z*1 conversion. The clusters showing *Z*2 conformation is highlighted in red (9.6 - 11.3%).

Figure S27. Contact plot per residue for the most probable cluster trajectories (Cn with percentage > 10) of KcsA−*Z*-LAB-TEA without K^+-ion resulting in *Z*1 and *Z*2 conformations, when LAB-TEA placed inside the channel cavity in *Z*2 conformation. Binding energy in kcal/mol is given in parenthesis. The SF, CC, and CG represent selectivity filter, channel cavity, and channel gate residues respectively.

Figure S28. Interaction of *Z*1 conformation with individual channel residues in the most probable conformation (C0), of the trajectory resulting in *Z*1, when simulation performed with *Z*-LAB-QA inside the channel cavity, without K^+-ion. The protein and *Z*1 represented as ribbon and stick (magenta) respectively, and the interacting residues THR-75 (red), ILE-100 (blue), PHE-103 (green), VAL-106 (ochre), and THR-107 (red) from extracellular to intracellular region in ball and stick model. The distances are given in Angstrom. Residue numbers are given in the upper left corner of each box.

Figure S29. Summary of hierarchical average-linkage clustering performed on trajectories of *E*-LAB-TEA without K^+-ion, when LAB-TEA placed inside the channel cavity. *E*a to *E*c are the starting structure for that particular trajectory. The average structure of each cluster is shown, indicating location of LAB-TEA relative to the ion channel. Cn (n = 0 − 4) indicates different clusters. Percentage occurrence of each cluster is given in parenthesis. Corresponding binding energy (B.E.) is given in kcal/mol. Protein is represented as new cartoon in the starting structure and as lines in the average structures. LAB-TEA is shown as a stick model. All the simulations retained the *E*1 binding poses as that in the starting structure.

Figure S30. Contact plot per residue for the most probable cluster trajectories (Cn with percentage > 10) of KcsA−*E*-LAB-TEA without K^+-ion resulting in *E*1 conformation, when LAB-TEA placed inside the channel cavity in *E*1 conformation. Binding energy in kcal/mol is given in parenthesis. The SF, CC, and CG represent selectivity filter, channel cavity, and channel gate residues respectively.

Figure S31. Summary of hierarchical average-linkage clustering performed on trajectories of *E*-LAB-TEA without K^+-ion, when LAB-TEA placed inside the channel cavity. *E*2a to *E*2e are the starting structure for that particular trajectory. The average structure of each cluster is shown, indicating location of LAB-TEA relative to the ion channel. Cn (n = 0−4) indicates different

clusters. Percentage occurrence of each cluster is given in parenthesis. Corresponding binding energy (B.E.) is given in kcal/mol. Protein is represented as new cartoon in the starting structure and as lines in the average structures. LAB-TEA is shown as a stick model. All the simulations retained the *E*2 binding poses as that in the starting structure.

Figure S32. Contact plot per residue for the most probable cluster trajectories (Cn with percentage > 10) of KcsA−*E*-LAB-TEA without K^+-ion resulting in *E*2 conformation, when LAB-TEA placed inside the channel cavity in *E*2 conformation. Binding energy in kcal/mol is given in parenthesis. The SF, CC, and CG represent selectivity filter, channel cavity, and channel gate residues respectively.

Figure S33. Interaction of (a) *E*1 and (b) *E*2 conformation with individual channel residues in the most probable conformation (C0), when simulation performed with *E*-LAB-TEA inside the channel cavity, without K^+-ion. The protein and *E*-LAB-TEA are represented as ribbon and stick (green) respectively, and the interacting residues THR-75 (red), ILE-100 (blue), PHE-103 (green), GLY- 104 (purple), VAL-106 (ochre), THR-107 (red), and LEU-110 (grey) from extracellular to the intracellular region in the ball and stick model. The distances are given in Angstrom. Residue numbers are given in the upper left corner of each box.

Figure S34. The structure of a) *E*1, b) *E*2, and c) *Z*1 corresponds to the first energy barrier in Figure 10, where *E*1(dark green), *E*2 (green), and *Z*1 (magenta) encounter the channel gate residues for the first time during their transition from the intracellular region. The KcsA channel is shown in ribbon and K^+-ion is shown as the purple ball.

Figure S35. The structure of a) *Z*1 corresponds to the energy 'dip' in the PMF plot, Figure 10. b) Possible interactions of LAB moiety of *Z*1 with the channel gate residues. The KcsA channel is shown in ribbon and K^+-ion is shown as the purple ball.

Supplementary Table Legend

Table S1. The calculated binding energy (ΔH) and entropy contribution (TΔS) using the molecular mechanics Poisson Boltzmann surface area (MMPBSA) and the Kongsted Ryde entropy methods respectively are given.

Supplementary Movie Legends

Movie S1. The trajectory of *Z*-LAB-TEA (licorice; cyan = carbon, blue = nitrogen, red = oxygen, and white = hydrogens) with KcsA channel (new cartoon model) in presence of K^+-ion (purple ball) showing that the curved nature of the LAB restricts *Z*-LAB-TEA movement into the CC. The residues THR-75 and THR-107 are shown in ball and stick model (red). This trajectory is part of 400 ns simulation on *Z*1a given in Figure S1.

Movie S2. The trajectory of *Z*-LAB-TEA (licorice; cyan = carbon, blue = nitrogen, red = oxygen, and white = hydrogens) with KcsA channel (new cartoon model) without K^+-ion showing the re-orientation of *Z*2 inside the cavity to *Z*1 during the 400 ns simulation on *Z*2a given in Figure S26. The residues THR-75 and THR-107 are shown in ball and stick model (red).

Movie S3. Trajectory showing *E*2 → *E*1 → *E*2 rotation of *E*-LAB-TEA (licorice; cyan = carbon, blue = nitrogen, red = oxygen, and white = hydrogens) outside the channel cavity (new cartoon model). The *E*2 exit the cavity and then enters as *E*1, again come out of the cavity and finally enters as *E*2. Th trajectory is part of the 100 ns on *E*2d given in Figure S1. The residues THR-75 and THR-107 are shown in ball and stick model (red). The K^+-ion represented as purple ball.

Movie S4. Trajectory showing possible rotation of *E*-LAB-TEA (licorice; cyan = carbon, blue = nitrogen, and white = hydrogens) from *E*1 to *E*2 outside the cavity (new cartoon model) and its entry as *E*2. This trajectory is part of 100 ns simulation on *E*1c given in Figure S1. The residues THR-75 and THR-107 are shown in ball and stick model (red). The K^+-ion represented as purple ball.

Movie S5. Simulation trajectory of *E*-LAB-TEA (licorice; cyan = carbon, blue = nitrogen, red = oxygen, and white = hydrogens) with K^+-ion (purple ball) inside the cavity (new cartoon model) shows prompt exit of *E*1 from the channel cavity. This trajectory is part of 100 ns simulation when a total of six simulations (three for each *E*1 and *E*2) performed on the KcsA-K^+-*E*-LAB-TEA systems. Out of the three simulations one is 400 ns and remaining two are 100 ns each). The residues THR-75 and THR-107 are shown in ball and stick model (red).

Supplementary Scheme S1

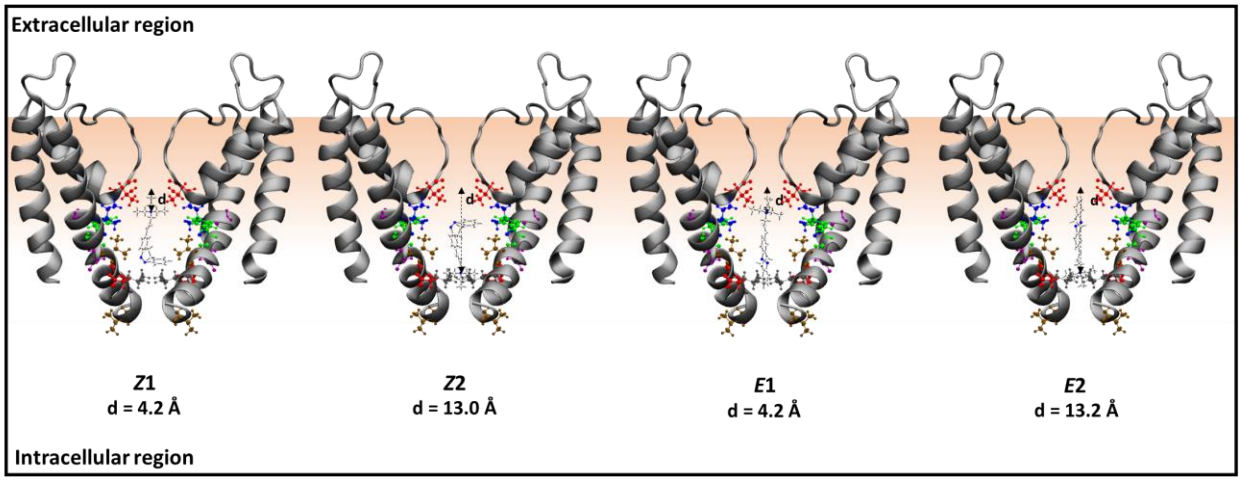

Scheme S1. Schematic representation of KcsA-LAB-TEA starting conformations used for the simulation without K^+-ion. The open KcsA (PDB ID: 3F5W) showing only two diagonally opposite subunits, and is represented as a new cartoon. The TEA and amino-acids represented by ball and stick model (red = threonine (THR-75 and THR-107), purple = glycine (GLY-99), blue = isoleucine (ILE-100), green = phenylalanine (PHE-103), ochre = valine (VAL-106 and VAL-115), grey = leucine (LEU-110)). The azo-nitrogens and TEA nitrogen are shown as blue in colour. The purple ball represents the potassium ion. And d represents the distance between the center of C_α of THR-75 and nitrogen of TEA.

Supplementary Figures S1-S35

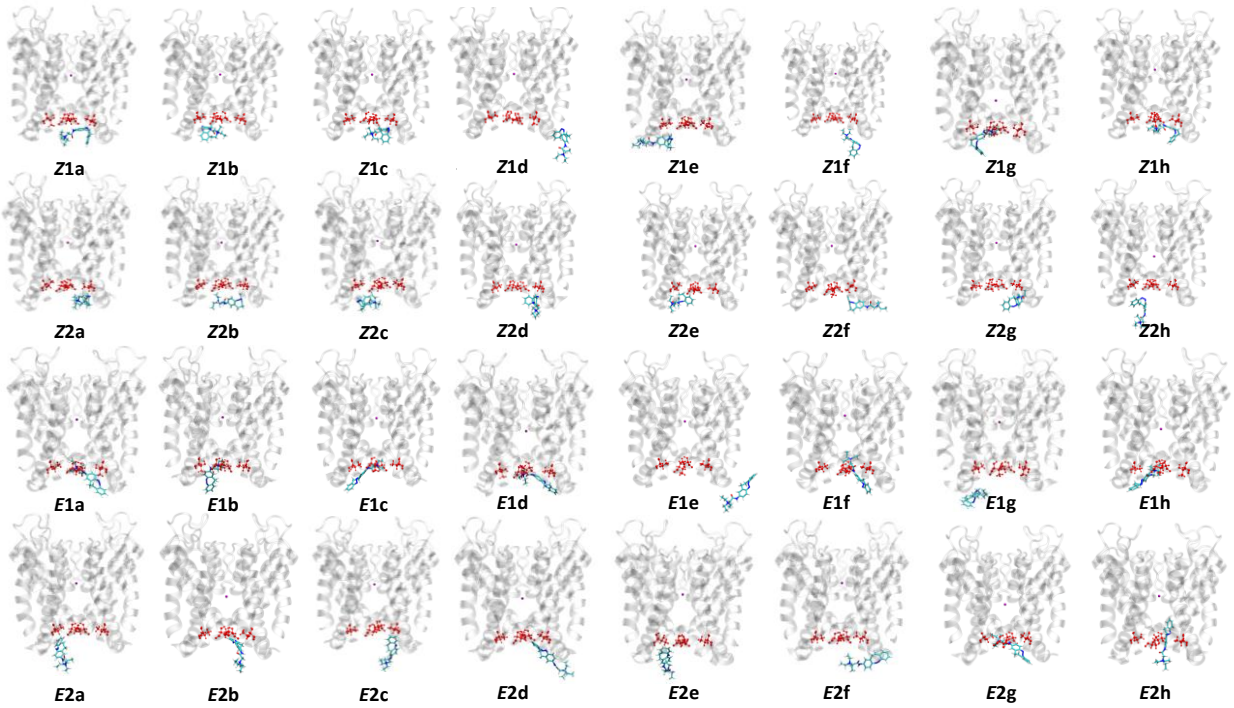

Figure S1. Starting structures resulted after equilibration for the molecular dynamics simulation of *Z*1 (*Z*1a-*Z*lh), *Z*2 (*Z*2a-*Z*2h), *E*1 (*E*1a-*E*lh) and *E*2-isomers (*E*2a-*E*2h) of LAB-TEA (stick model) with KcsA-K^+-ion channel (new cartoon representation in grey colour) with one K^+-ion (purple ball). LAB-TEA is in the cytoplasmic region. The amino-acid residue THR-107 (red) shown in ball and stick model. Note that we have not studied the dynamics of $Z \leftrightarrow E$ photo-isomerization inside the potassium ion channel directly. All the structures were subjected to 100 ns simulation except *Z*1a, *Z*2a, *E*1a, and *E*2a (400 ns).

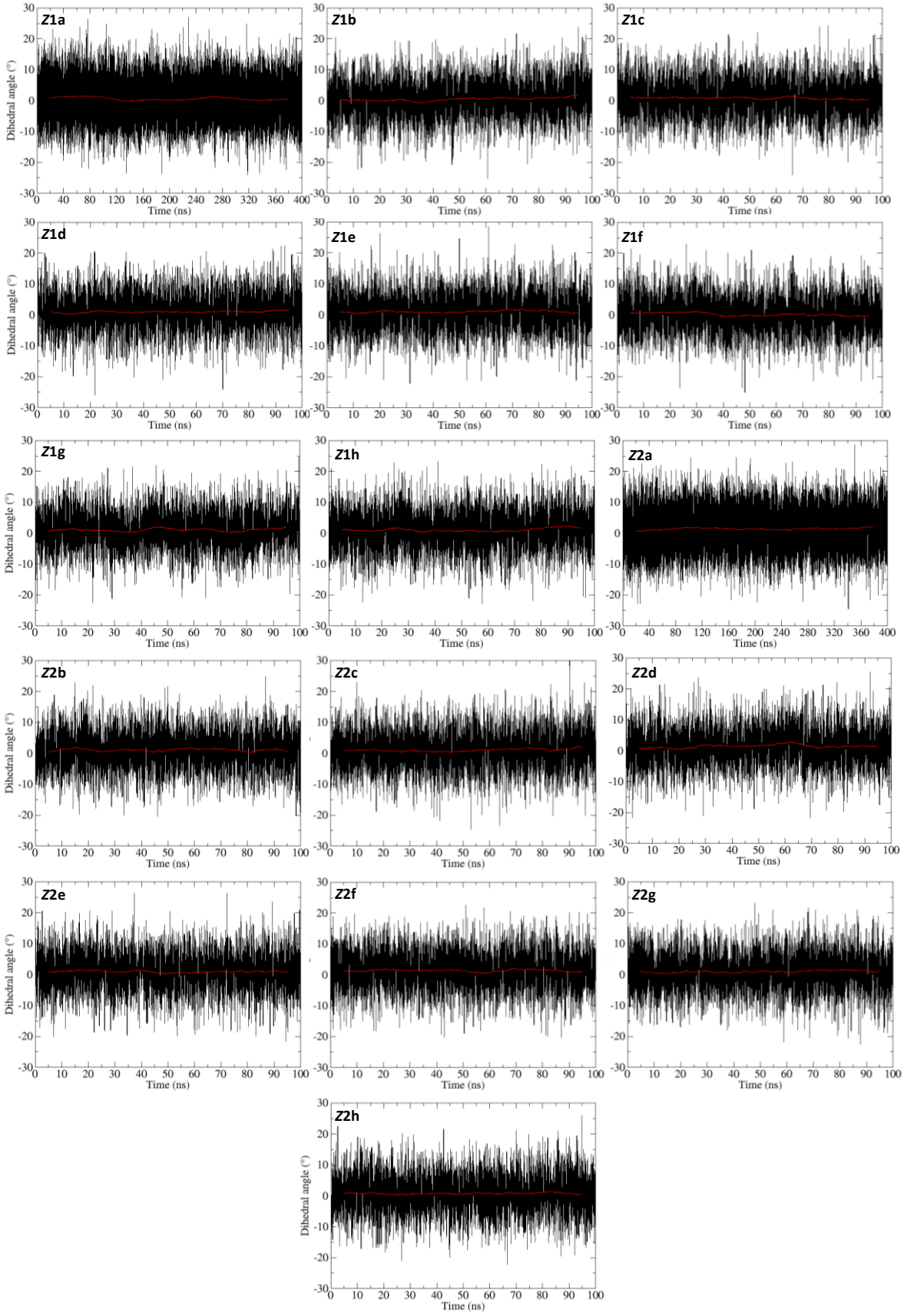
Z1a
Z1b
Z1c
Z1d
Z1e
Z1f
Z1g
Z1h
Z2a
Z2b
Z2c
Z2d
Z2e
Z2f
Z2g
Z2h
Dihedral angle (°)
Time (ns)

Figure S2. Dihedral angle plot (Time (ns) vs. Dihedral angle (degree)) for *Z*-LAB-TEA when placed in the cytoplasmic region during simulation with one K^+-ion. The red line represents the average dihedral angle in degrees.

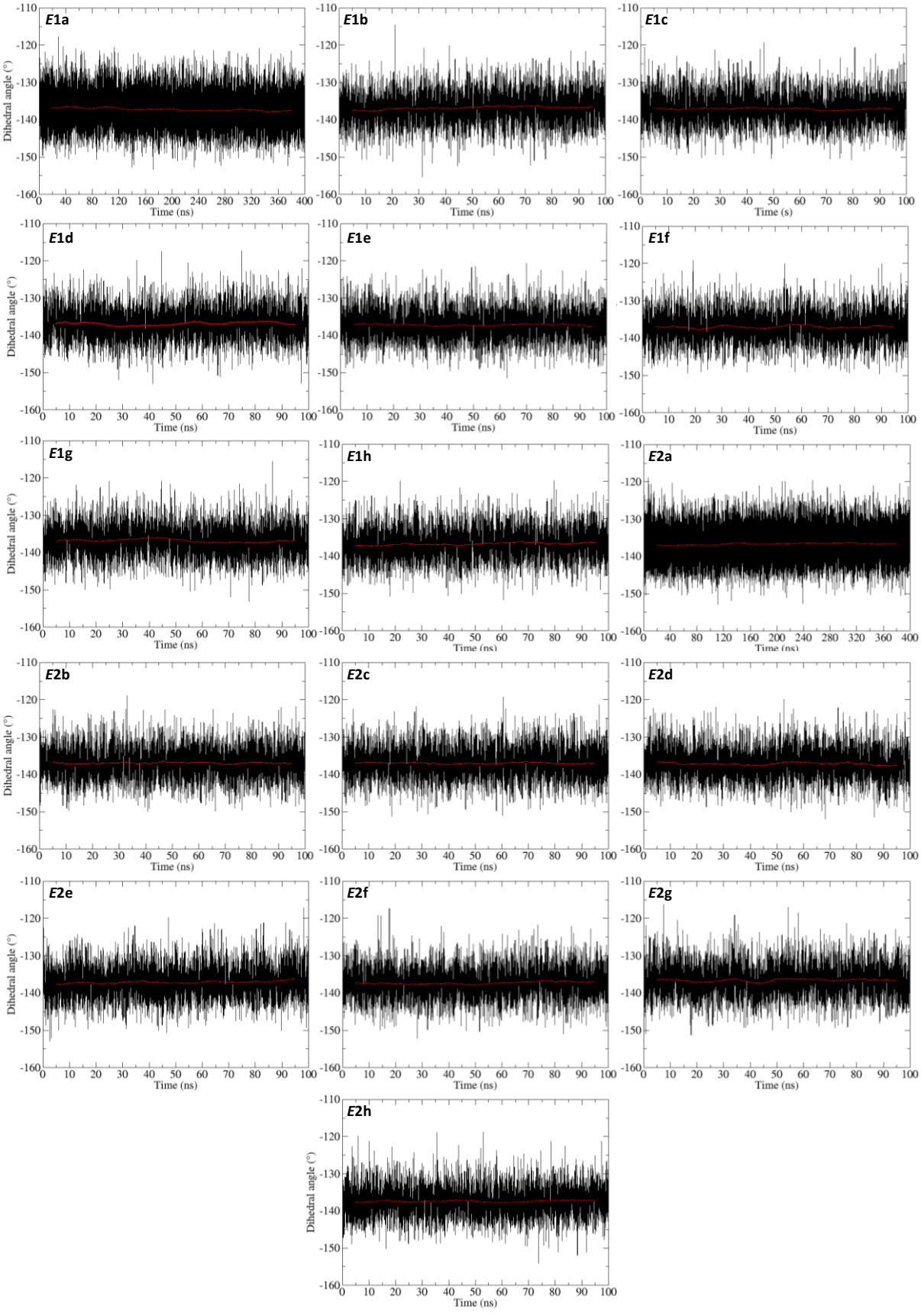
E1a
E1b
E1c
E1d
E1e
E1f
E1g
E1h
E2a
E2b
E2c
E2d
E2e
E2f
E2g
E2h
Dihedral angle (°)
Time (ns)
Time (s)

Figure S3. Dihedral angle plot (Time (ns) vs. Dihedral angle (degree)) for *E*-LAB-TEA when placed in the cytoplasmic region during simulation with one K^+-ion. The red line represents the average dihedral angle in degrees.

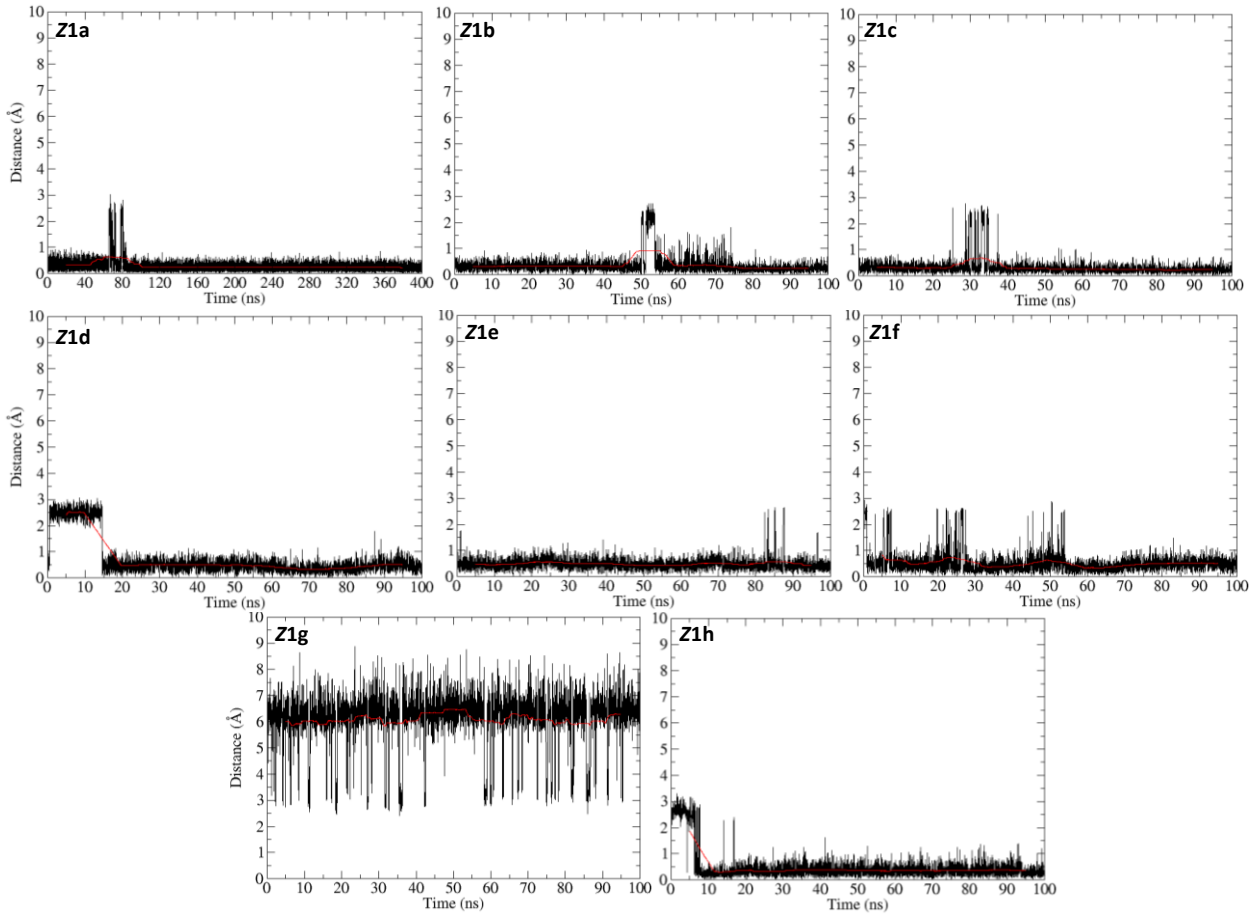

Figure S4. Distance plot (Time (ns) vs. Distance (Å)) showing variation in the K^+-$C_{\alpha THR\text{-}75}$ distances during the simulations started with *Z*1 with one K^+-ion. The red line represents the average value in Angstrom.

Note: The profile of *Z*1g differs from the rest because the simulation of *Z*1g was performed with a restraint of 0.5 kcal/mol/Å^2 on the K^+ ion. The observed deviation in K^+-$C_{\alpha THR\text{-}75}$ distances results from the possible electrostatic repulsion between the positively charged K^+-ion and TEA moiety. It also indicates that the binding of LAB-TEA to the channel cavity would displace the K^+-ions. The profile for Z2 (1.5%) was not obtained due to its scant presence in the channel cavity.

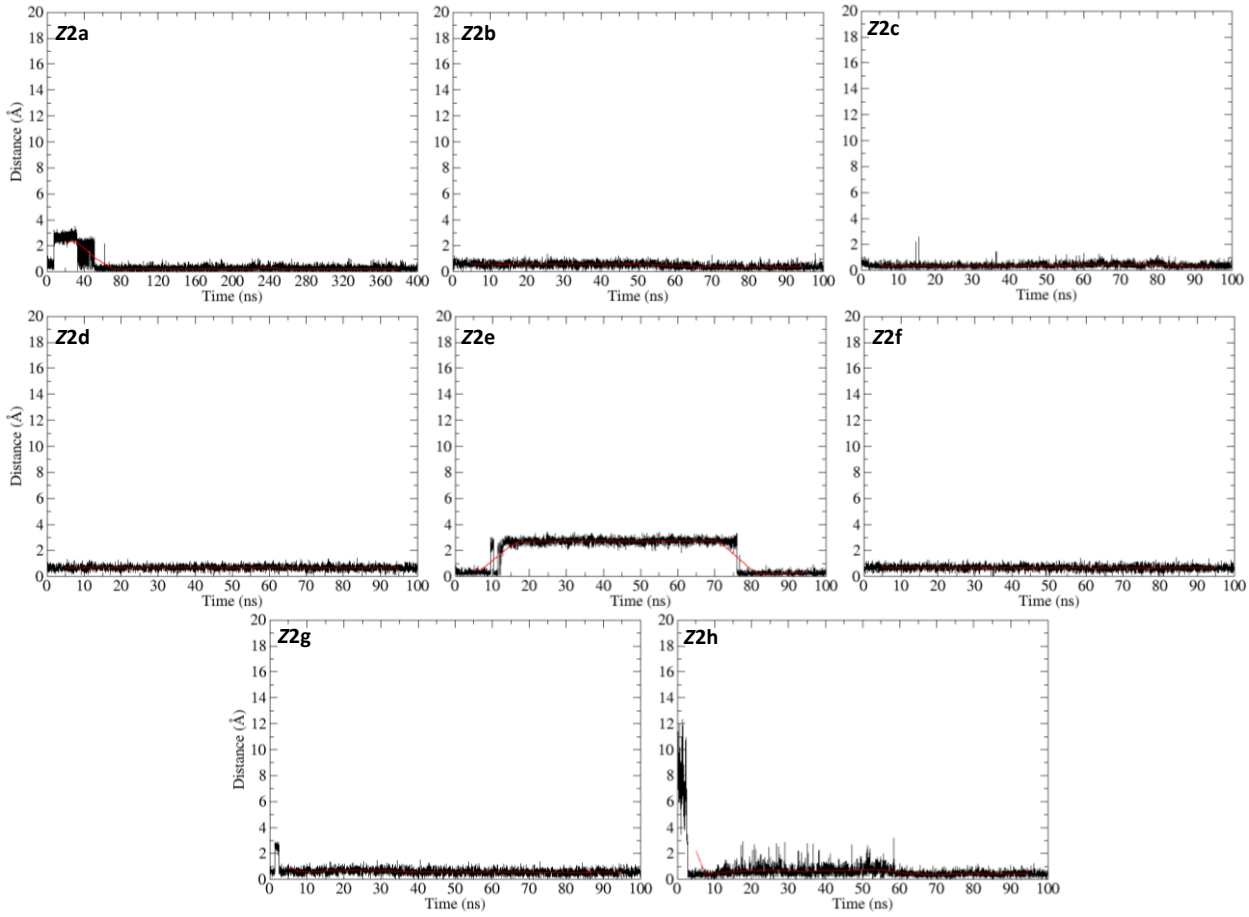

Figure S5. Distance plot (Time (ns) vs. Distance (Å)) showing variation in the K^+-$C_{\alpha THR-75}$ distances during the simulations started with *Z*2 with one K^+-ion. The red line represents the average value in Angstrom.

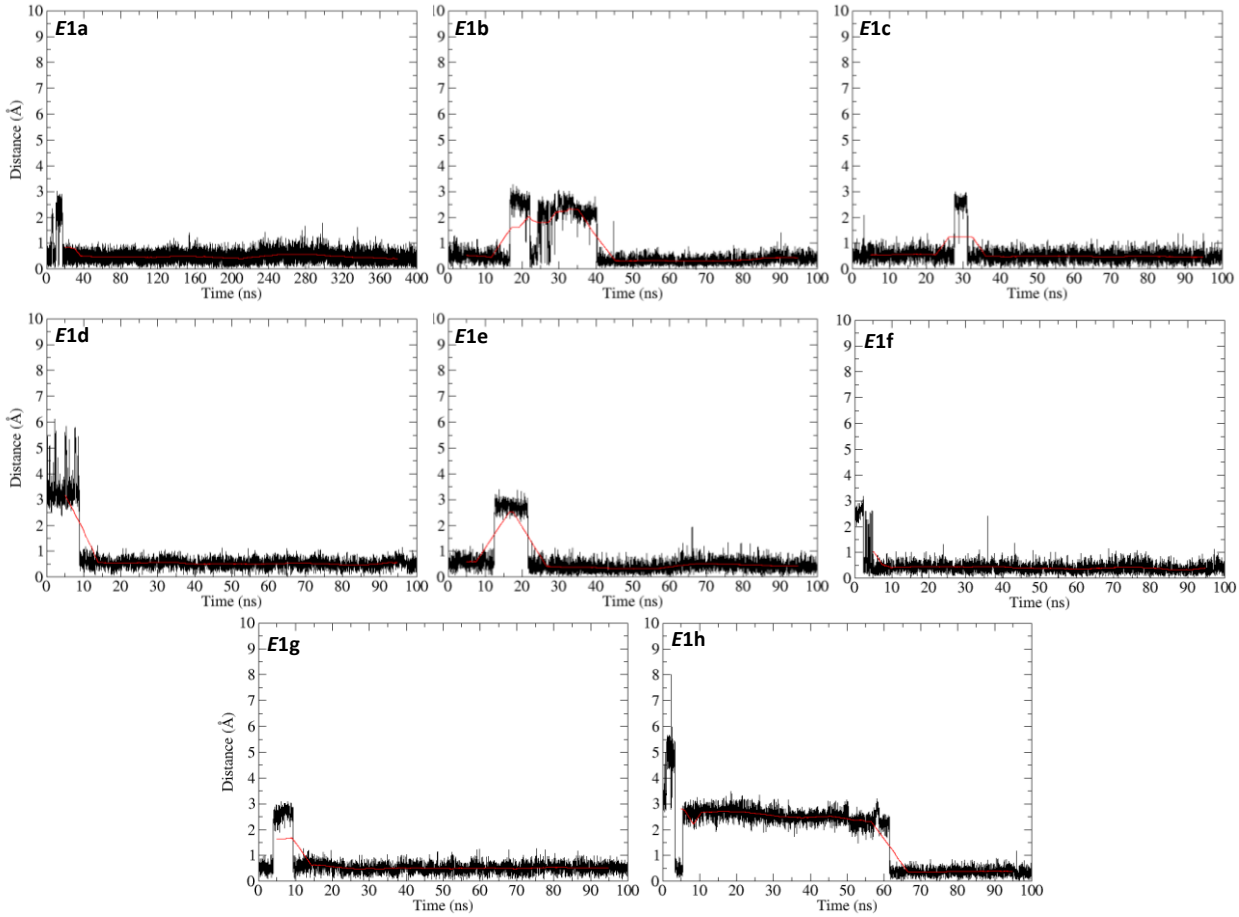

Figure S6. Distance plot (Time (ns) vs. Distance (Å)) showing variation in the K^+-$C_{\alpha THR-75}$ distances during the simulations started with *E*1 with one K^+-ion. The red line represents the average value in Angstrom.

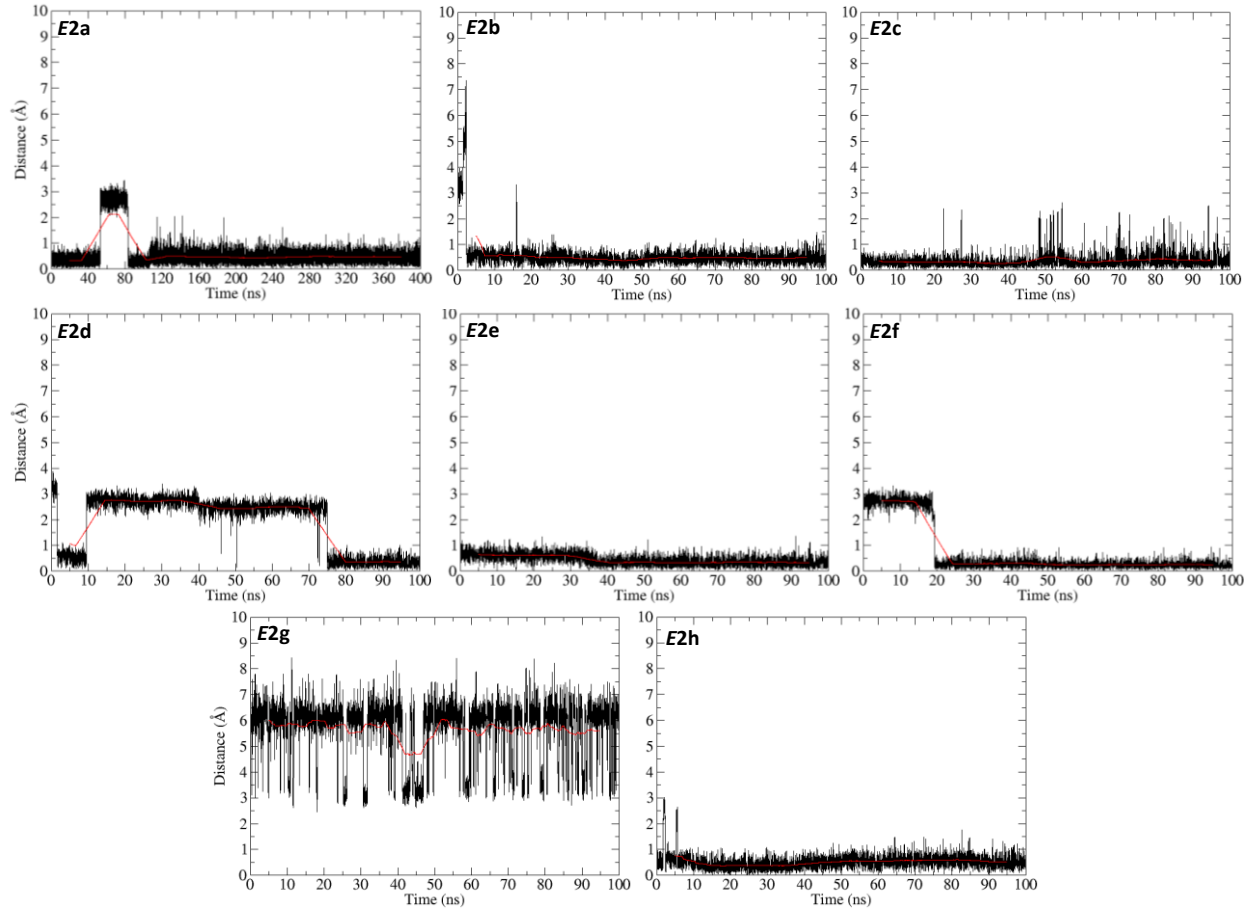

Figure S7. Distance plot (Time (ns) vs. Distance (Å)) showing variation in the K^+-$C_{\alpha THR-75}$ distances during the simulations started with *E*2 with one K^+-ion. The red line represents the average value in Angstrom.

Note: The profile of *E*2g differs from the rest because the simulation of *E*2g was performed with a restraint of 0.5 kcal/mol/Å² on the K^+-ion. The observed deviation in K^+-$C_{\alpha THR-75}$ distances results from the possible electrostatic interaction between the positively charged K^+-ion and LAB moiety. It also, indicates that the binding of LAB-TEA to the channel cavity would displace the K^+-ions. The profile for *E*1 (0.0%) was not obtained due to its scant presence in the channel cavity simultaneously with the K^+ ion. (**Movie S5**).

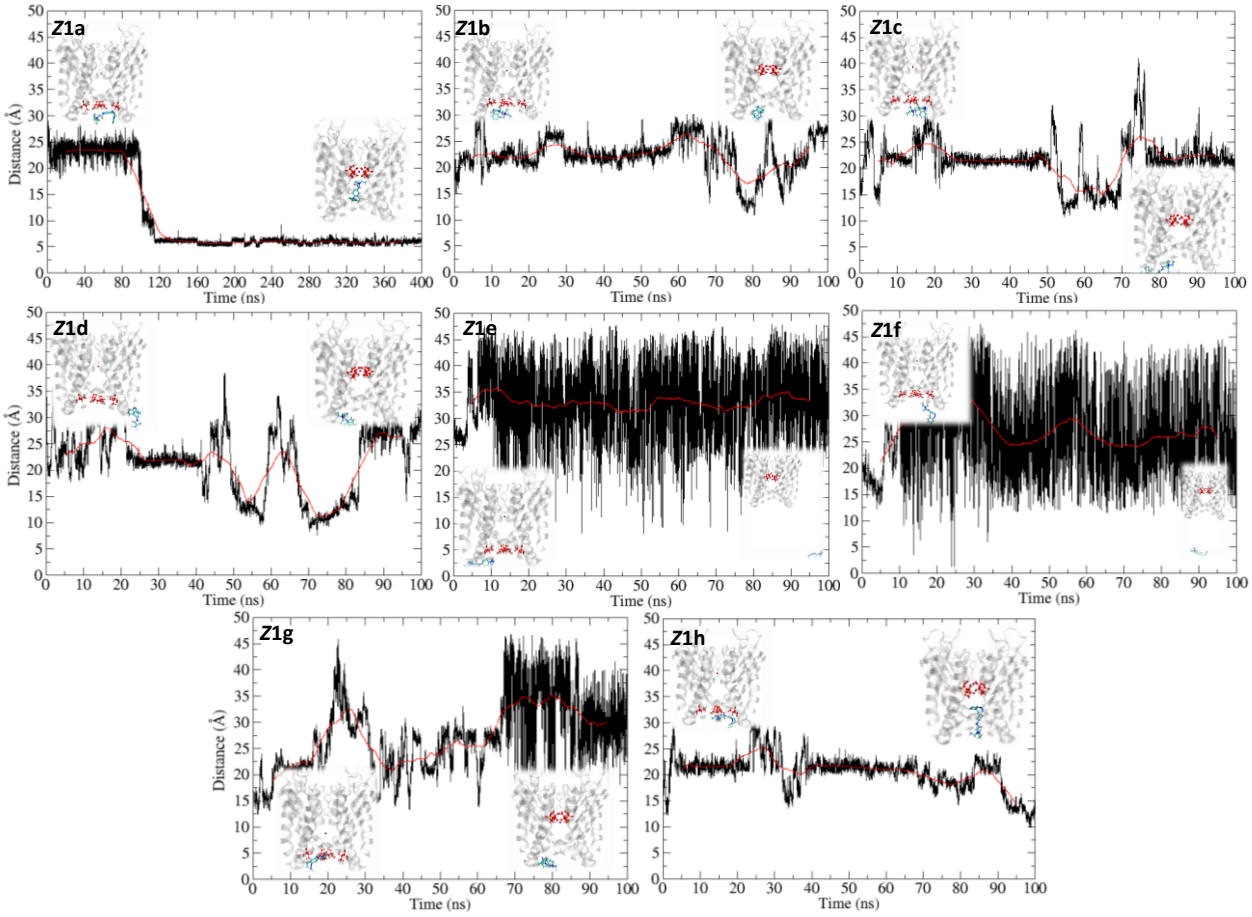

Figure S8. Distance plot (Time (ns) vs. Distance (Å)) showing variation in the $_{TEA}N\text{-}C_{\alpha THR\text{-}75}$ distances during the simulations started with *Z*1 with one K^+-ion. The red line represents the average value in Angstrom. The starting position and the preferable position of LAB-TEA during the simulation are shown in left and right insets, respectively.

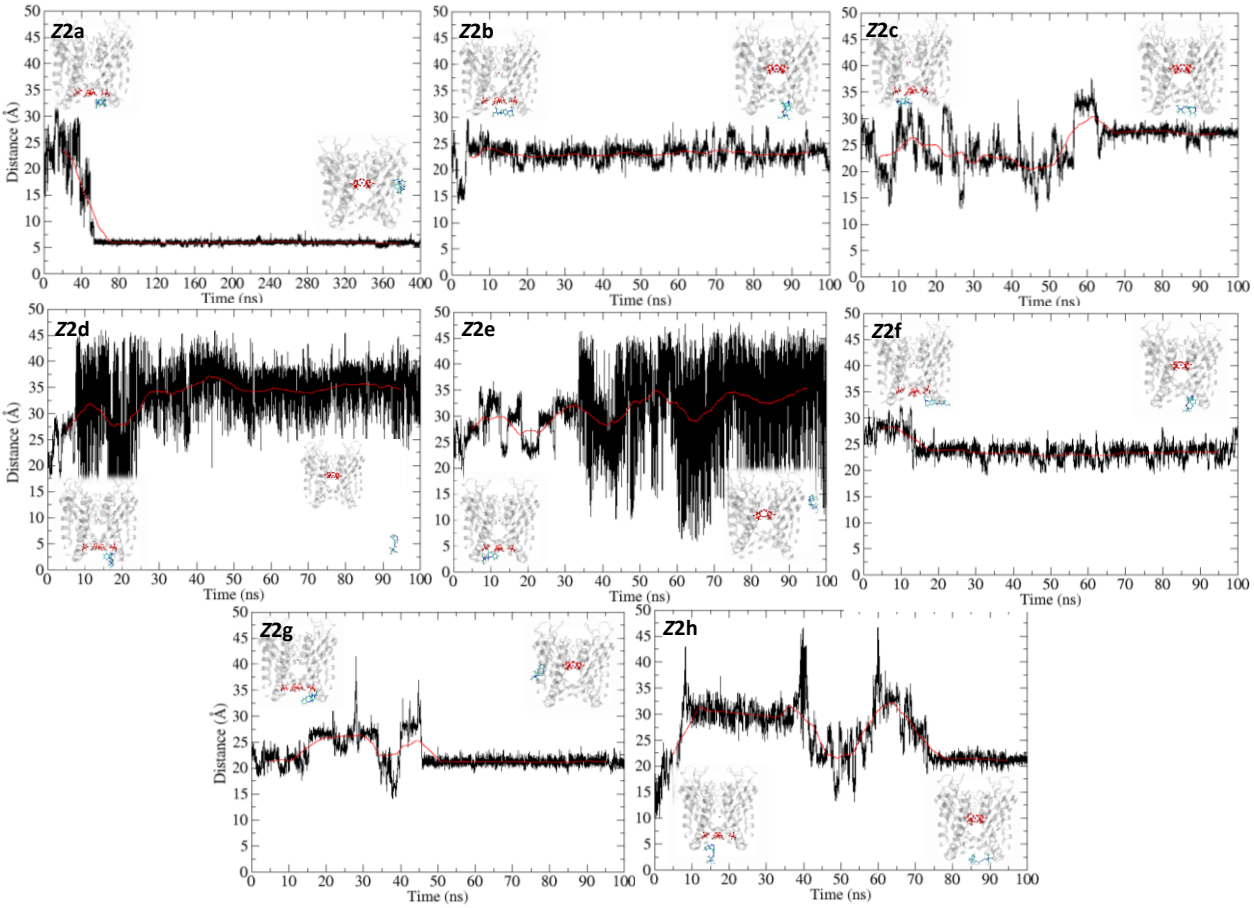

Figure S9. Distance plot (Time (ns) vs. Distance (Å)) showing variation in the $_{TEA}N\text{-}C_{\alpha THR\text{-}75}$ distances during the simulations started with *Z*2 with one K^+-ion. The red line represents the average value in Angstrom. The starting position and the preferable position of LAB-TEA during the simulation shown in left and right insets, respectively.

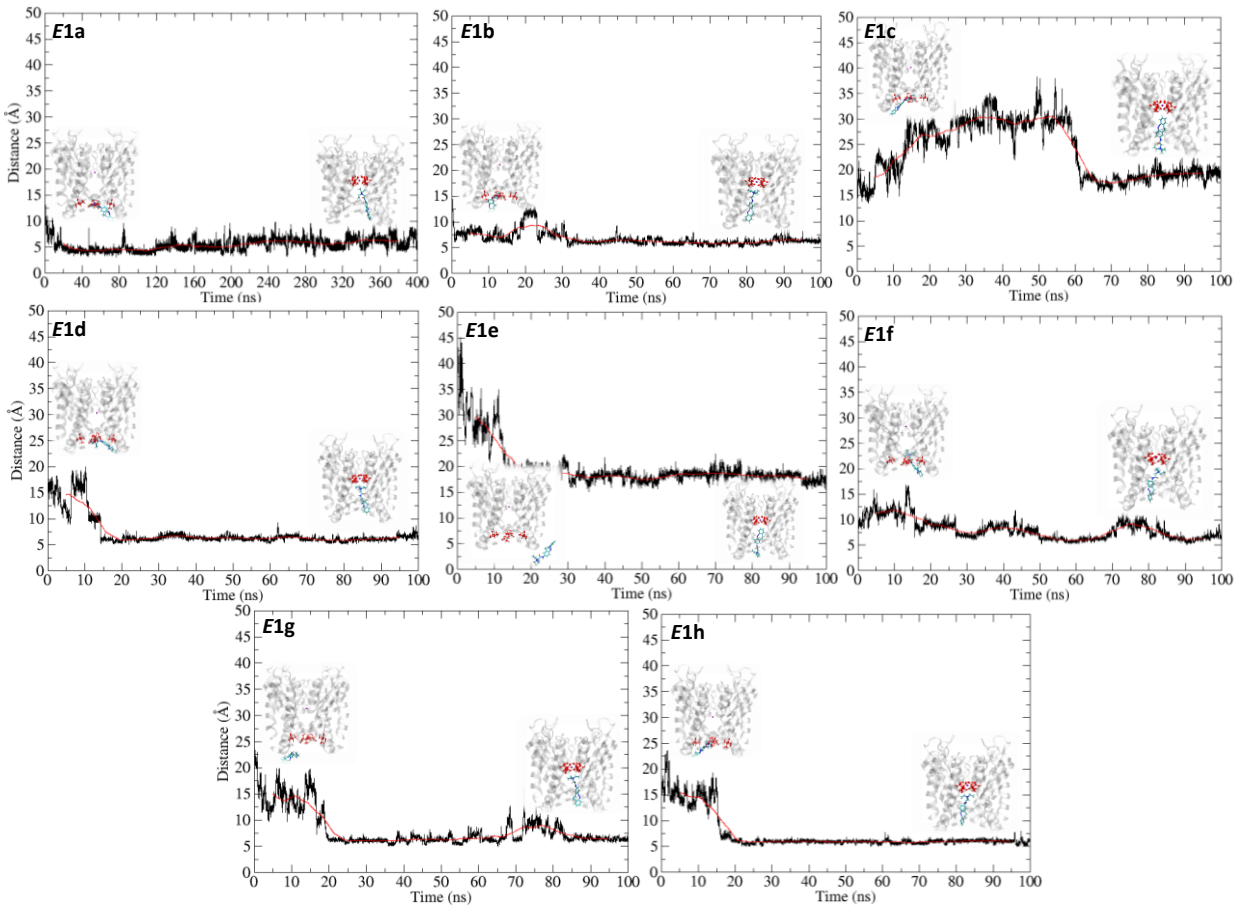

Figure S10. Distance plot (Time (ns) vs. Distance (Å)) showing variation in the $_{TEA}N\text{-}C_{\alpha THR\text{-}75}$ distances during the simulations started with *E*1 with one K^+-ion. The red line represents the average value in Angstrom. The starting position and the preferable position of LAB-TEA during the simulation are shown in left and right insets, respectively.

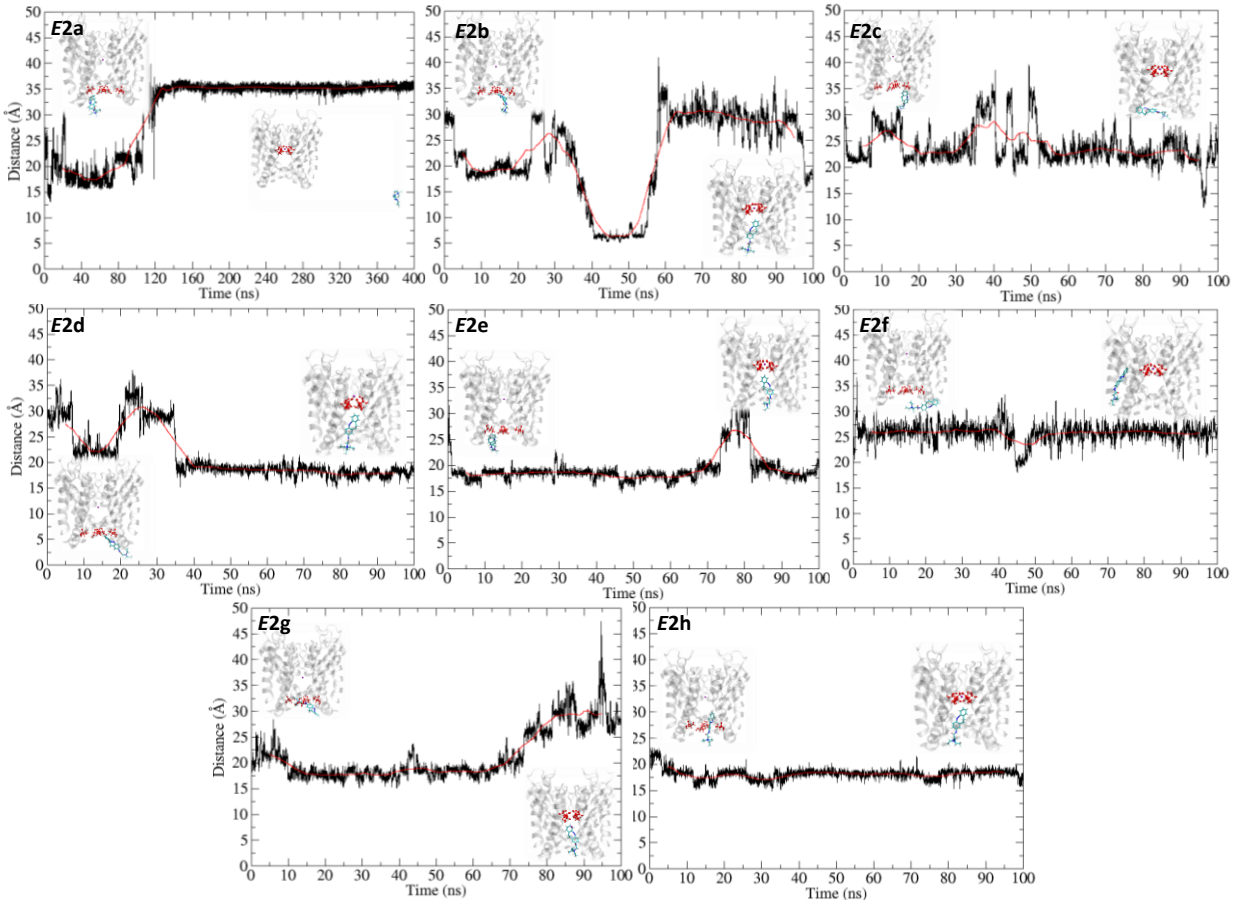

Figure S11. Distance plot (Time (ns) vs. Distance (Å)) showing variation in the $_{TEA}N\text{-}C_{\alpha THR\text{-}75}$ distances during the simulations started with *E*2 with one K^+-ion. The red line represents the average value in Angstrom. The starting position and the preferable position of LAB-TEA during the simulation are shown in left and right insets, respectively.

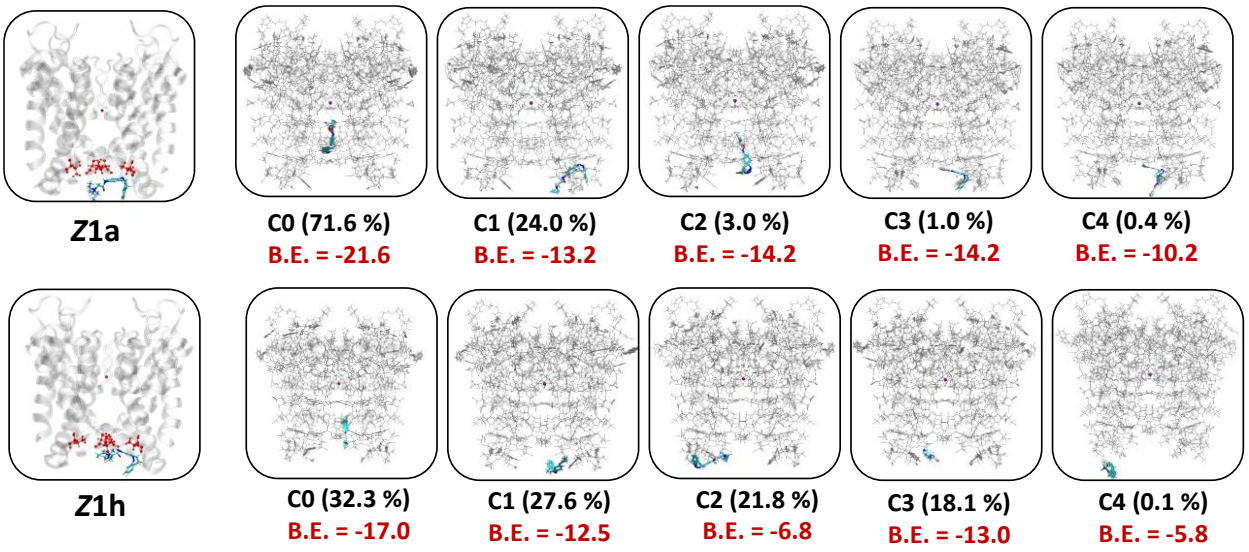

Figure S12. Summary of hierarchical average-linkage clustering performed on trajectories of *Z*-LAB-TEA with one K^+-ion (purple ball) showing binding of *Z*-isomer into the channel cavity, when LAB-TEA placed in the cytoplasmic region. *Z*1a and *Z*1h are the starting structures resulting in *Z*1 and *Z*2 binding conformations respectively. The average structure of each cluster is shown, indicating location of LAB-TEA relative to the ion channel. Cn (n = 0 − 4) indicates different clusters. Percentage occurrence of each cluster is given in parenthesis. Corresponding binding energy (B.E.) is given in kcal/mol. Protein is represented as new cartoon in the starting structure and as lines in the average structures. LAB-TEA is shown as a stick model.

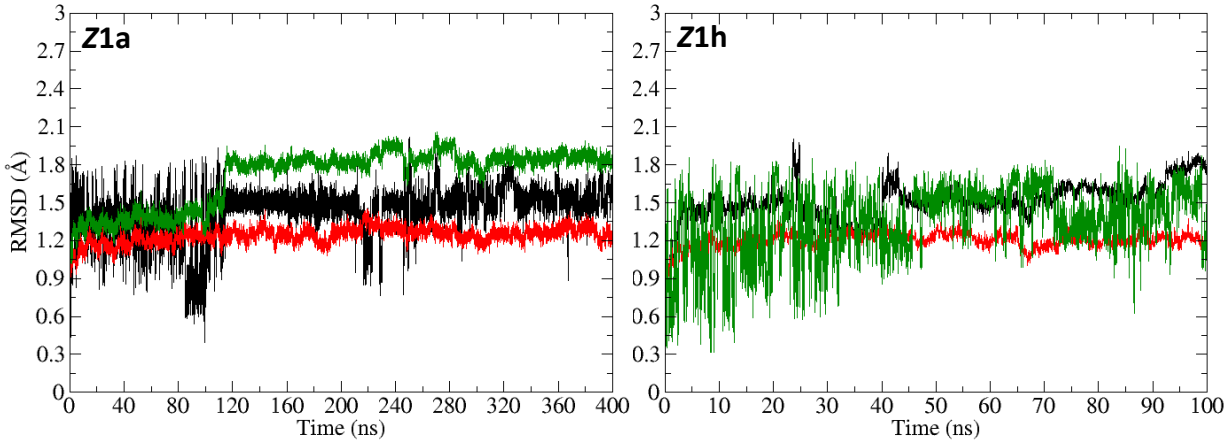

Figure S13. Root-mean-square deviation plot (Time (ns) vs. RMSD (Å)) for *Z*-LAB-TEA with one K^+-ion resulting in the entry of *Z*-isomer to the channel cavity, when LAB-TEA placed in the cytoplasmic region. *Z*1a and *Z*1h are the starting structure for that particular trajectory resulting in *Z*1 and *Z*2 respectively. Black, red, and green graphs show RMSD of KcsA with *Z*-LAB-TEA, KcsA alone, and *Z*-LAB-TEA alone respectively.

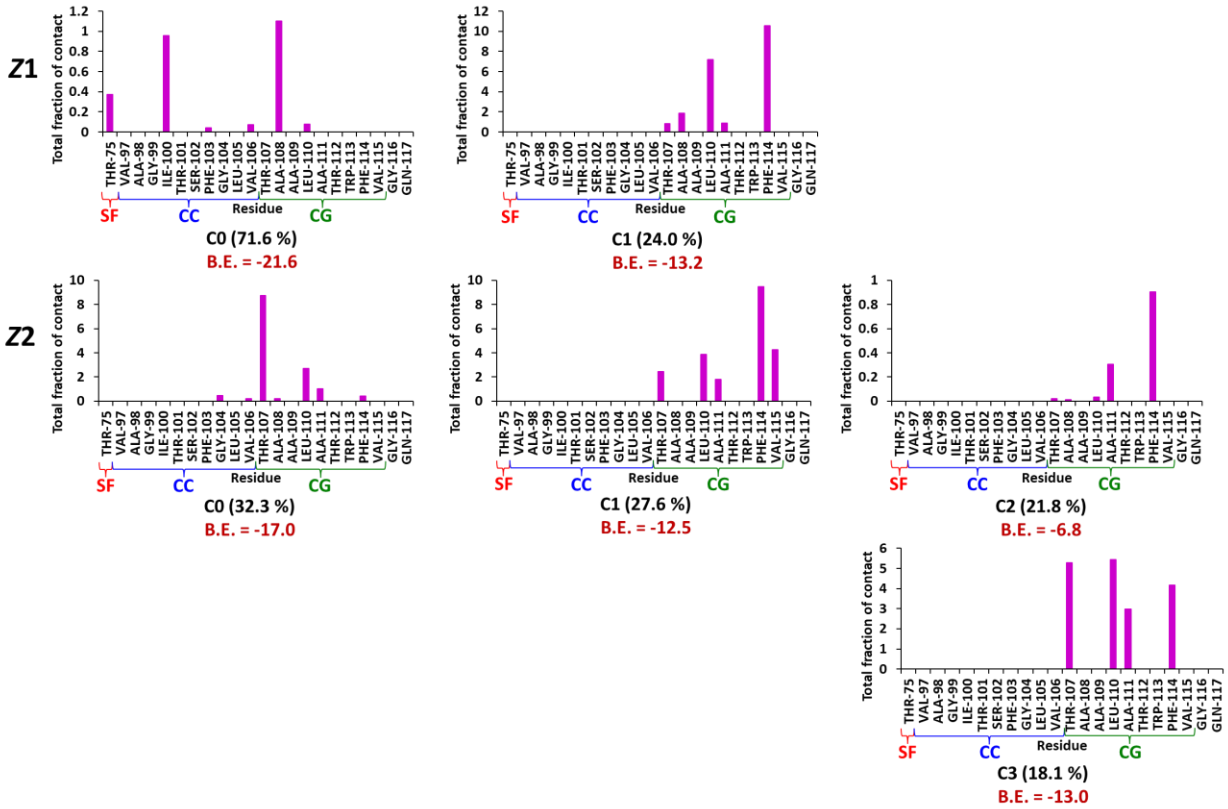

Figure S14. Contact plot per residue for the most probable cluster trajectories (Cn with percentage > 10) of KcsA−*Z*-LAB-TEA with K^+-ion resulting in *Z*1 and *Z*2 conformations, when LAB-TEA placed in the cytoplasmic region. Binding energy in kcal/mol is given in parenthesis. The SF, CC, and CG represent selectivity filter, channel cavity, and channel gate residues respectively.

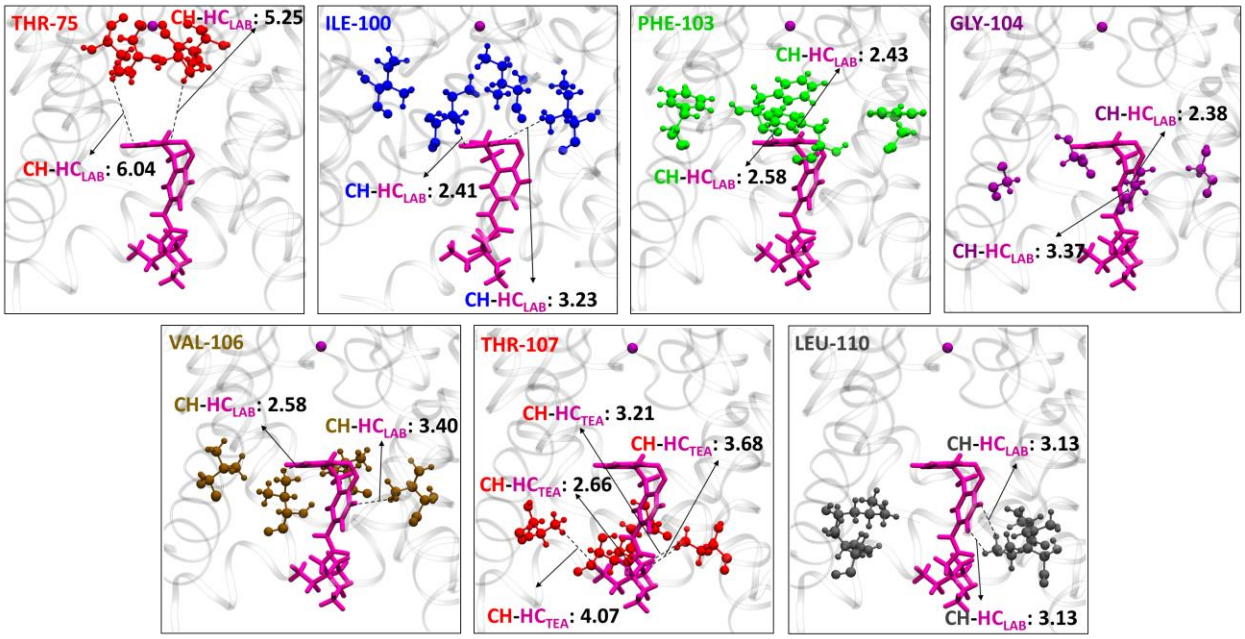

Figure S15. Interaction of *Z*2 conformation with individual channel residues in the most probable conformation (C0), of the trajectory resulting in *Z*-entry to the KcsA channel cavity, when simulation performed with one K^+-ion (purple ball model) inside the channel and *Z*-LAB-QA in the cytoplasmic region. The protein and *Z*2 represented as ribbon and stick (magenta) respectively, and the interacting residues THR-75 (red), ILE-100 (blue), PHE-103 (green), GLY- 104 (purple), and THR-107 (red) from extracellular to intracellular region in ball and stick model. The distances are given in Angstrom. Residue numbers are given in the upper left corner of each box.

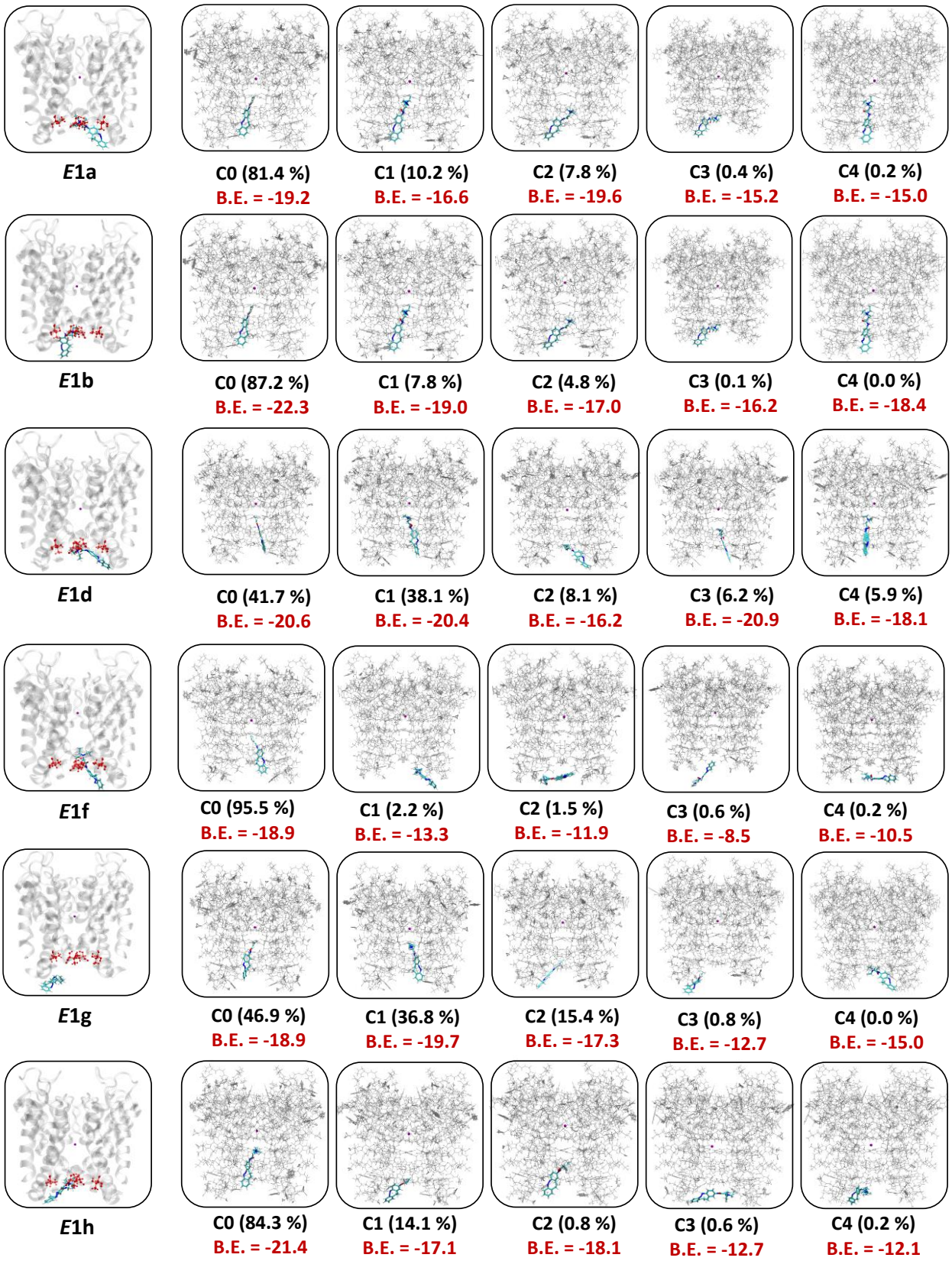
*E*1a
C0 (81.4 %)
B.E. = -19.2
C1 (10.2 %)
B.E. = -16.6
C2 (7.8 %)
B.E. = -19.6
C3 (0.4 %)
B.E. = -15.2
C4 (0.2 %)
B.E. = -15.0
*E*1b
C0 (87.2 %)
B.E. = -22.3
C1 (7.8 %)
B.E. = -19.0
C2 (4.8 %)
B.E. = -17.0
C3 (0.1 %)
B.E. = -16.2
C4 (0.0 %)
B.E. = -18.4
*E*1d
C0 (41.7 %)
B.E. = -20.6
C1 (38.1 %)
B.E. = -20.4
C2 (8.1 %)
B.E. = -16.2
C3 (6.2 %)
B.E. = -20.9
C4 (5.9 %)
B.E. = -18.1
*E*1f
C0 (95.5 %)
B.E. = -18.9
C1 (2.2 %)
B.E. = -13.3
C2 (1.5 %)
B.E. = -11.9
C3 (0.6 %)
B.E. = -8.5
C4 (0.2 %)
B.E. = -10.5
*E*1g
C0 (46.9 %)
B.E. = -18.9
C1 (36.8 %)
B.E. = -19.7
C2 (15.4 %)
B.E. = -17.3
C3 (0.8 %)
B.E. = -12.7
C4 (0.0 %)
B.E. = -15.0
*E*1h
C0 (84.3 %)
B.E. = -21.4
C1 (14.1 %)
B.E. = -17.1
C2 (0.8 %)
B.E. = -18.1
C3 (0.6 %)
B.E. = -12.7
C4 (0.2 %)
B.E. = -12.1

Figure S16. Summary of hierarchical average-linkage clustering performed on trajectories of *E*-LAB-TEA with one K^+-ion (purple ball) showing entry of *E*-isomer into the channel cavity, when LAB-TEA placed in the cytoplasmic region, and resulting in *E*1 conformation. Structures *E*1a to *E*1h are the starting structure for that particular trajectory. The average structure of each cluster is shown, indicating location of LAB-TEA relative to the ion channel. Cn (n = 0 − 4) indicates different clusters. Percentage occurrence of each cluster is given in parenthesis. Corresponding binding energy (B.E.) is given in kcal/mol. Protein is represented as new cartoon in the starting structure and as lines in the average structures. LAB-TEA is shown as a stick model.

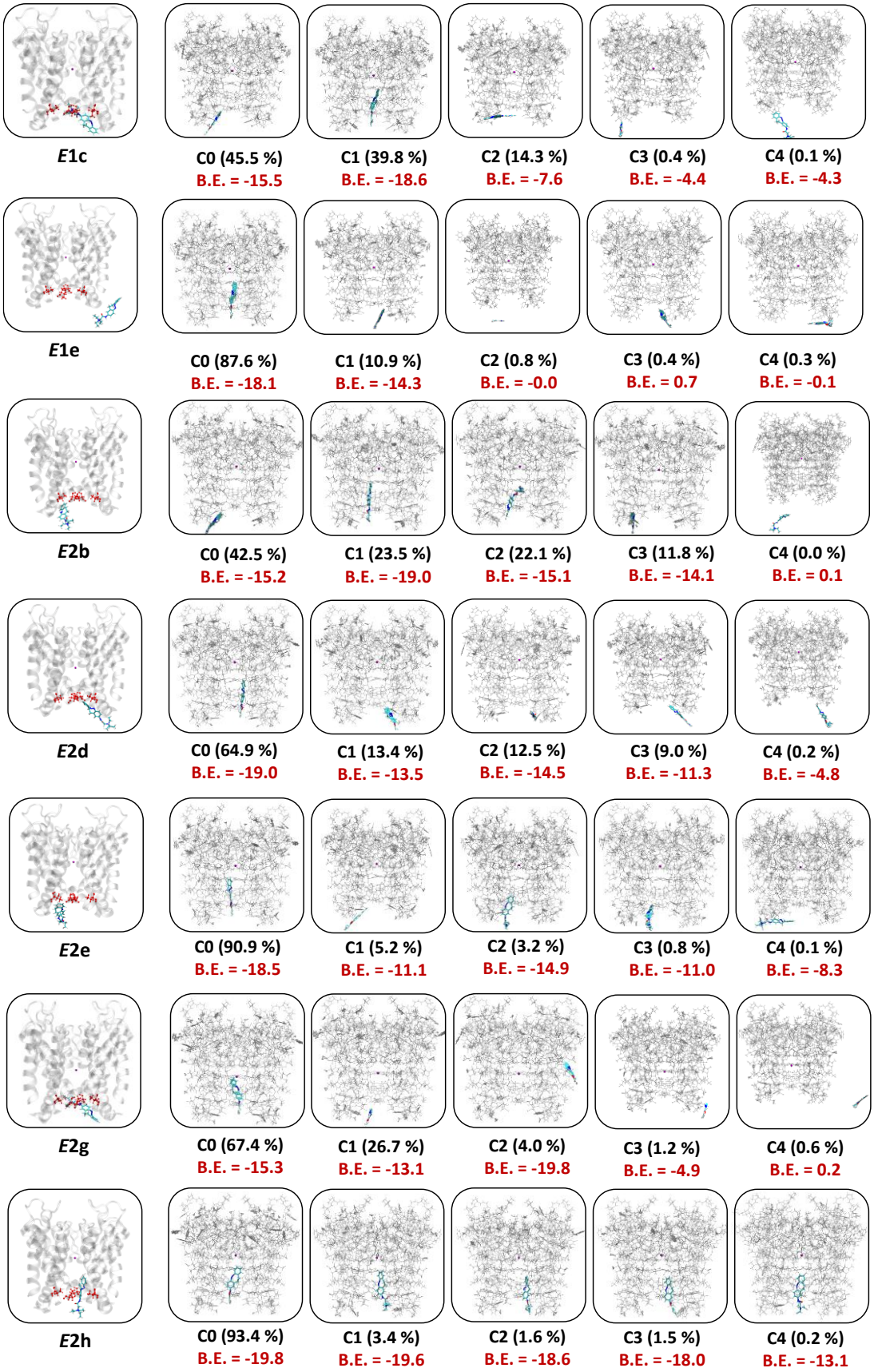
E1c
C0 (45.5 %)
B.E. = -15.5
C1 (39.8 %)
B.E. = -18.6
C2 (14.3 %)
B.E. = -7.6
C3 (0.4 %)
B.E. = -4.4
C4 (0.1 %)
B.E. = -4.3
E1e
C0 (87.6 %)
B.E. = -18.1
C1 (10.9 %)
B.E. = -14.3
C2 (0.8 %)
B.E. = -0.0
C3 (0.4 %)
B.E. = 0.7
C4 (0.3 %)
B.E. = -0.1
E2b
C0 (42.5 %)
B.E. = -15.2
C1 (23.5 %)
B.E. = -19.0
C2 (22.1 %)
B.E. = -15.1
C3 (11.8 %)
B.E. = -14.1
C4 (0.0 %)
B.E. = 0.1
E2d
C0 (64.9 %)
B.E. = -19.0
C1 (13.4 %)
B.E. = -13.5
C2 (12.5 %)
B.E. = -14.5
C3 (9.0 %)
B.E. = -11.3
C4 (0.2 %)
B.E. = -4.8
E2e
C0 (90.9 %)
B.E. = -18.5
C1 (5.2 %)
B.E. = -11.1
C2 (3.2 %)
B.E. = -14.9
C3 (0.8 %)
B.E. = -11.0
C4 (0.1 %)
B.E. = -8.3
E2g
C0 (67.4 %)
B.E. = -15.3
C1 (26.7 %)
B.E. = -13.1
C2 (4.0 %)
B.E. = -19.8
C3 (1.2 %)
B.E. = -4.9
C4 (0.6 %)
B.E. = 0.2
E2h
C0 (93.4 %)
B.E. = -19.8
C1 (3.4 %)
B.E. = -19.6
C2 (1.6 %)
B.E. = -18.6
C3 (1.5 %)
B.E. = -18.0
C4 (0.2 %)
B.E. = -13.1

Figure S17. Summary of hierarchical average-linkage clustering performed on trajectories of *E*-LAB-TEA with one K^+-ion (purple ball) showing entry of *E*-isomer into the channel cavity, when LAB-TEA placed in the cytoplasmic region, resulting in *E*2 conformation. *E*1c to *E*2h are the starting structure for that particular trajectory. The average structure of each cluster is shown, indicating the location of LAB-TEA relative to the ion channel. Cn (n = 0 − 4) indicates different clusters. Percentage occurrence of each cluster is given in parenthesis. Corresponding binding energy (B.E.) is given in kcal/mol. Protein is represented as new cartoon in the starting structure and as lines in the average structures. LAB-TEA is shown as a stick model.

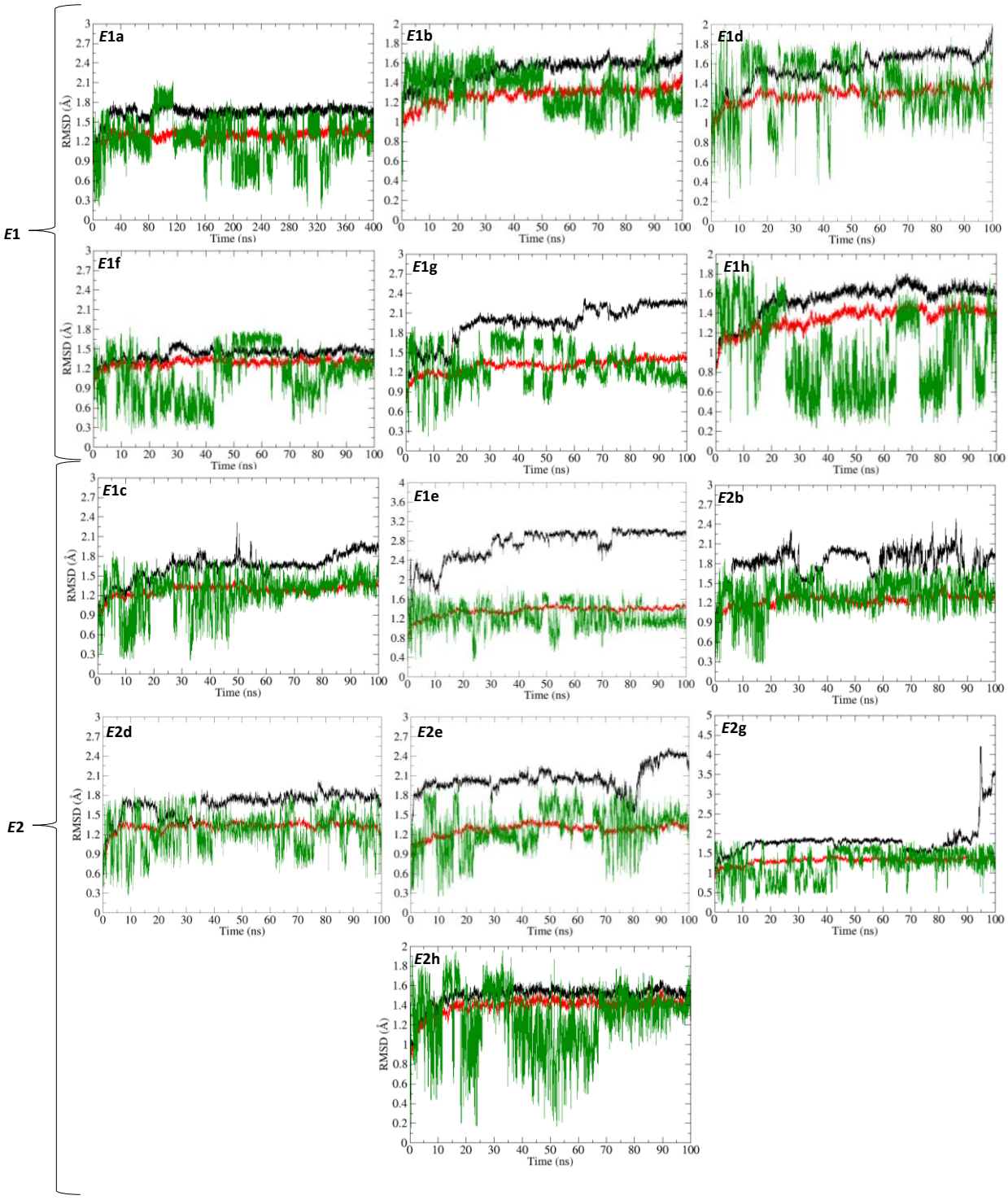

Figure S18. Root-mean-square deviation plot (Time (ns) vs. RMSD (Å)) for *E*-LAB-TEA with one K^+-ion resulting entry of *E*-isomer to the channel cavity, when LAB-TEA placed in the cytoplasmic region. *E*1a to *E*2h are the starting structure for that particular trajectory. Black, red, and green graphs show RMSD of KcsA with *E*-LAB-TEA, KcsA alone, and *E*-LAB-TEA alone respectively. The red line represents the average value in Angstrom.

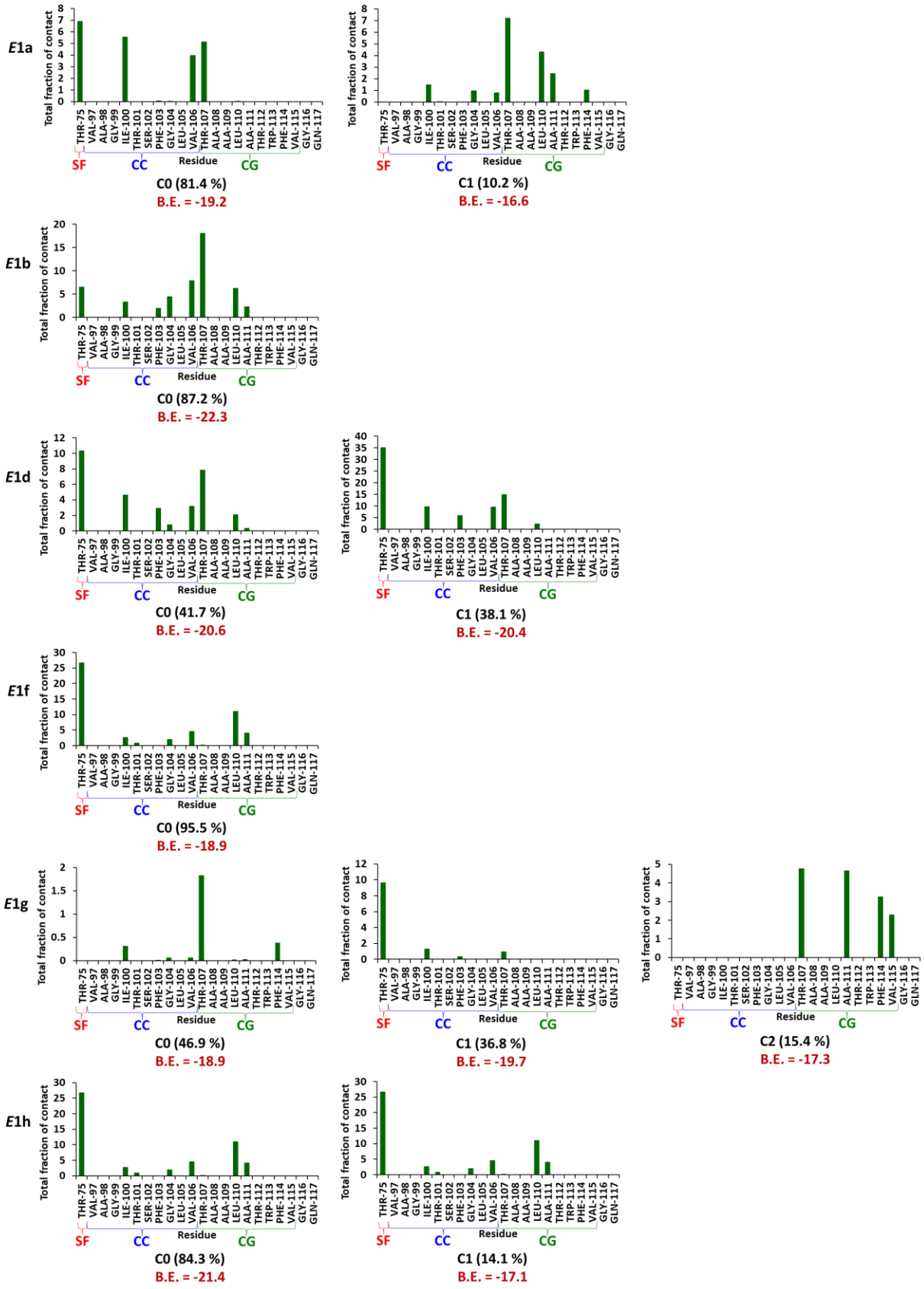
E1a
C0 (81.4 %)
B.E. = -19.2
C1 (10.2 %)
B.E. = -16.6
E1b
C0 (87.2 %)
B.E. = -22.3
E1d
C0 (41.7 %)
B.E. = -20.6
C1 (38.1 %)
B.E. = -20.4
E1f
C0 (95.5 %)
B.E. = -18.9
E1g
C0 (46.9 %)
B.E. = -18.9
C1 (36.8 %)
B.E. = -19.7
C2 (15.4 %)
B.E. = -17.3
E1h
C0 (84.3 %)
B.E. = -21.4
C1 (14.1 %)
B.E. = -17.1
Total fraction of contact
Residue
SF
CC
CG

Figure S19. Contact plot per residue for the most probable cluster trajectories (Cn with percentage > 10) of KcsA−*E*-LAB-TEA with K^+-ion resulting in *E*1 (*E*1a, *E*1b, *E*1d, *E*1f, *E*1g, and *E*1h) conformation, when LAB-TEA placed in the cytoplasmic region. Binding energy in kcal/mol is given in parenthesis. The SF, CC, and CG represent selectivity filter, channel cavity, and channel gate residues respectively.

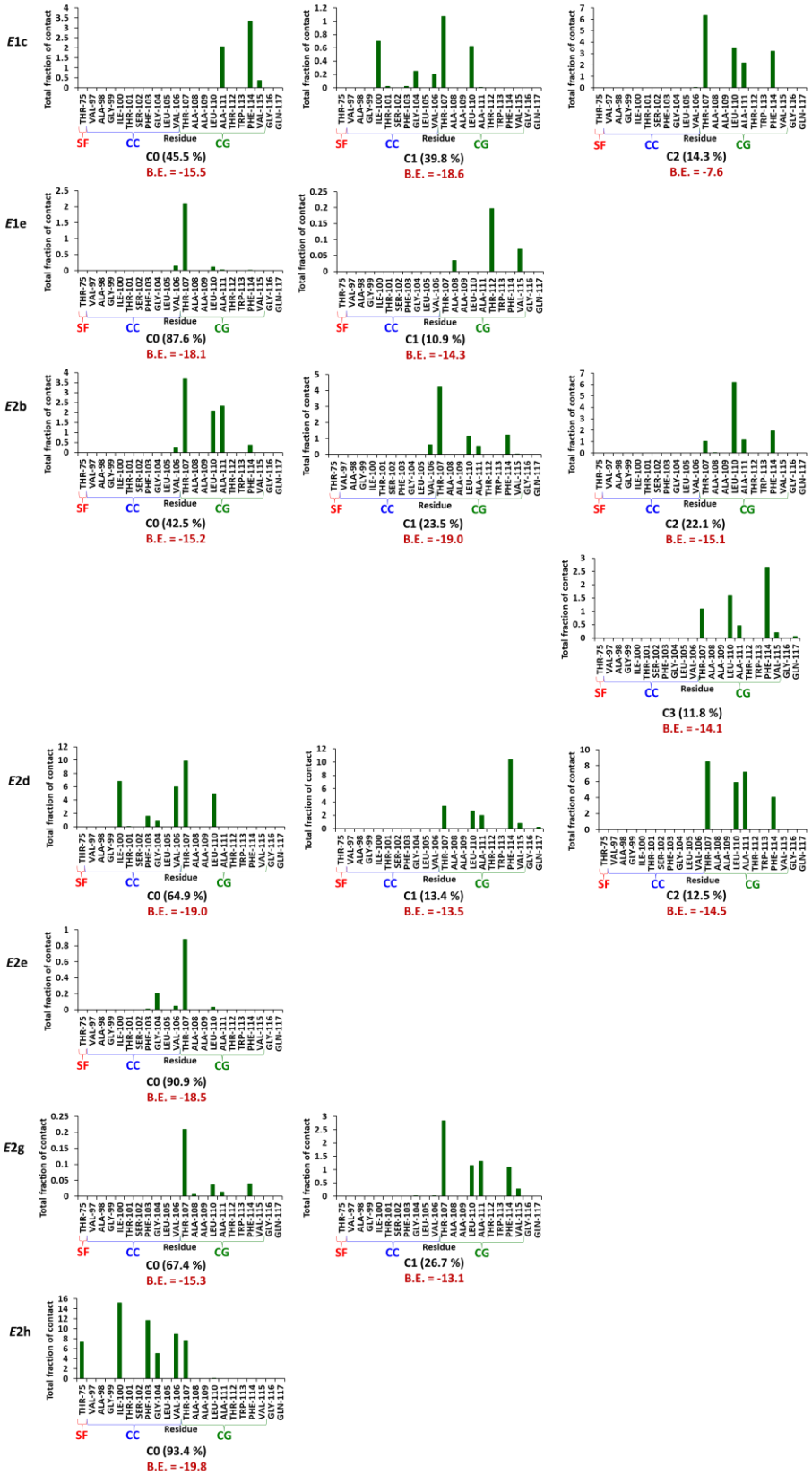
E1c
C0 (45.5 %)
B.E. = -15.5
C1 (39.8 %)
B.E. = -18.6
C2 (14.3 %)
B.E. = -7.6
E1e
C0 (87.6 %)
B.E. = -18.1
C1 (10.9 %)
B.E. = -14.3
E2b
C0 (42.5 %)
B.E. = -15.2
C1 (23.5 %)
B.E. = -19.0
C2 (22.1 %)
B.E. = -15.1
C3 (11.8 %)
B.E. = -14.1
E2d
C0 (64.9 %)
B.E. = -19.0
C1 (13.4 %)
B.E. = -13.5
C2 (12.5 %)
B.E. = -14.5
E2e
C0 (90.9 %)
B.E. = -18.5
E2g
C0 (67.4 %)
B.E. = -15.3
C1 (26.7 %)
B.E. = -13.1
E2h
C0 (93.4 %)
B.E. = -19.8
Total fraction of contact
Residue
SF
CC
CG

Figure S20. Contact plot per residue for the most probable cluster trajectories (Cn with percentage > 10) of KcsA−*E*-LAB-TEA with K^+-ion resulting in *E*2 conformation, when LAB-TEA placed in the cytoplasmic region. Binding energy in kcal/mol is given in parenthesis. The SF, CC, and CG represent selectivity filter, channel cavity, and channel gate residues respectively.

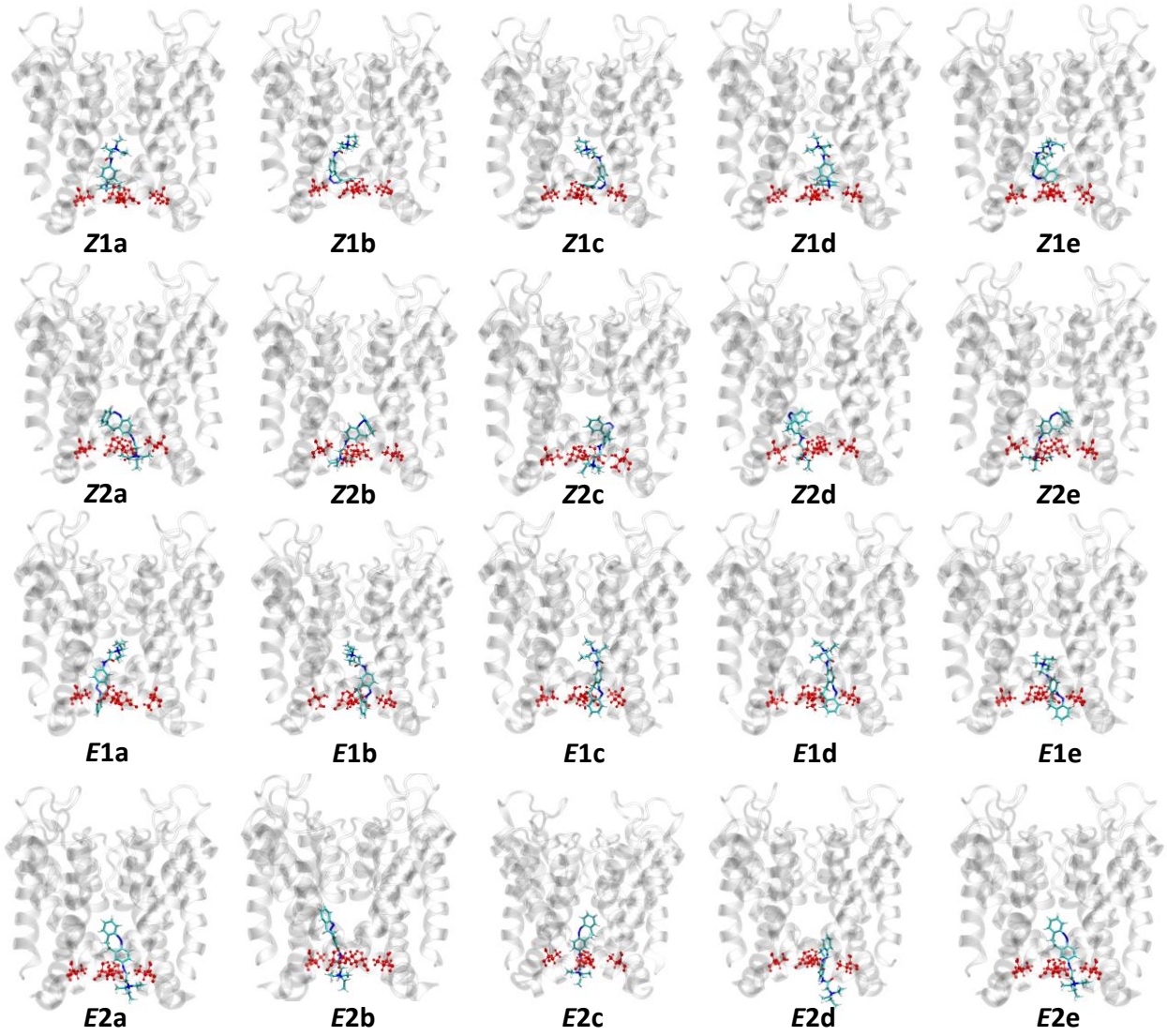

Figure S21. Starting structures for the molecular dynamics simulation of *Z*- and *E*-isomers of LAB-TEA (stick model) with KcsA-K^+-ion channel (new cartoon representation in grey colour) in the absence of K^+-ion. The LAB-TEA is inside the channel. The amino-acid residue THR-107 (red) shown in ball and stick model.

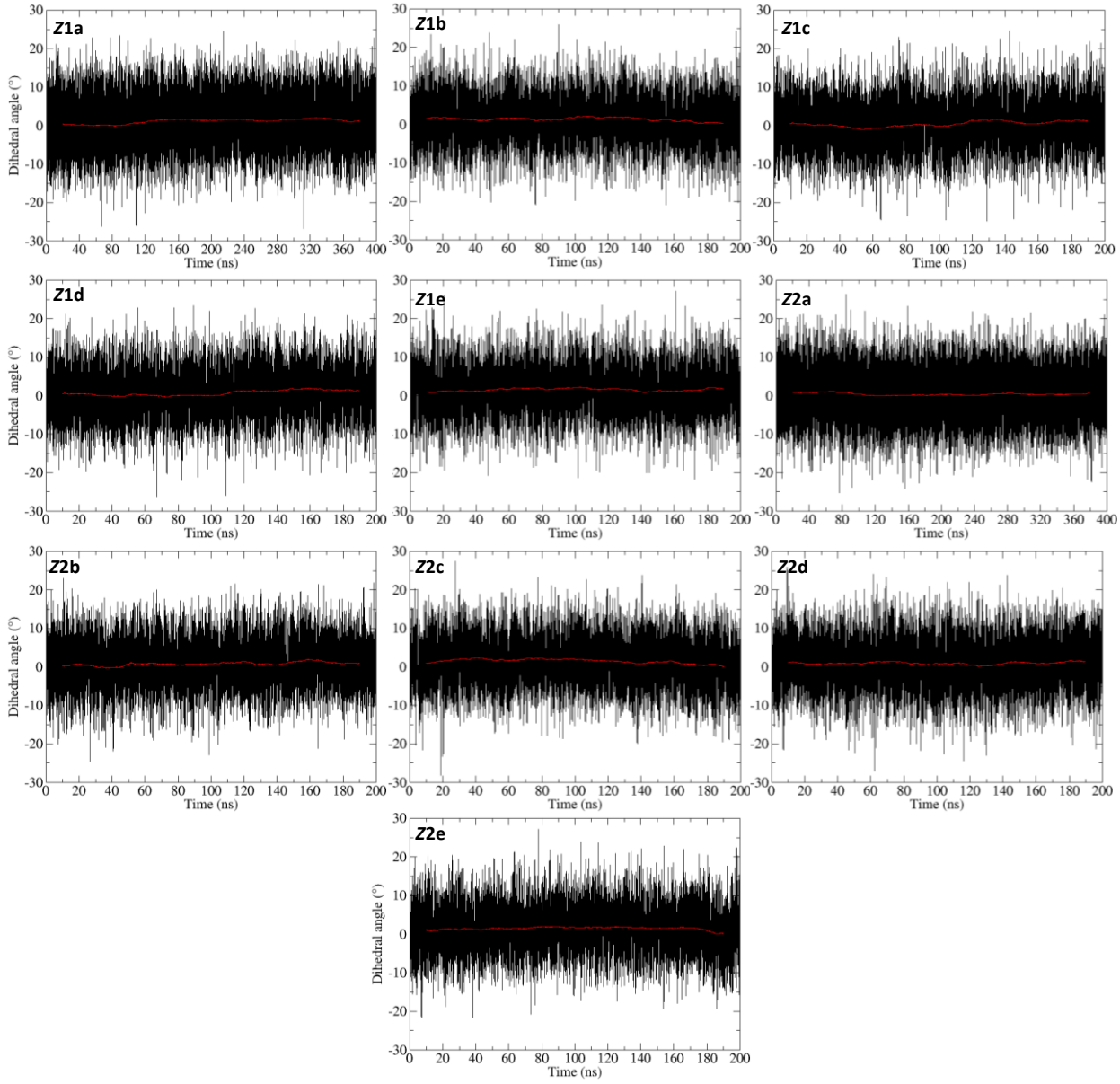

Figure S22. Dihedral angle plot (Time (ns) vs. Dihedral angle (degree)) for *Z*-LAB-TEA when placed inside the channel during simulation without K^+-ion. *Z*1a to *Z*2e represent the starting structure for that particular trajectory. The red line represents the average dihedral angle in degrees.

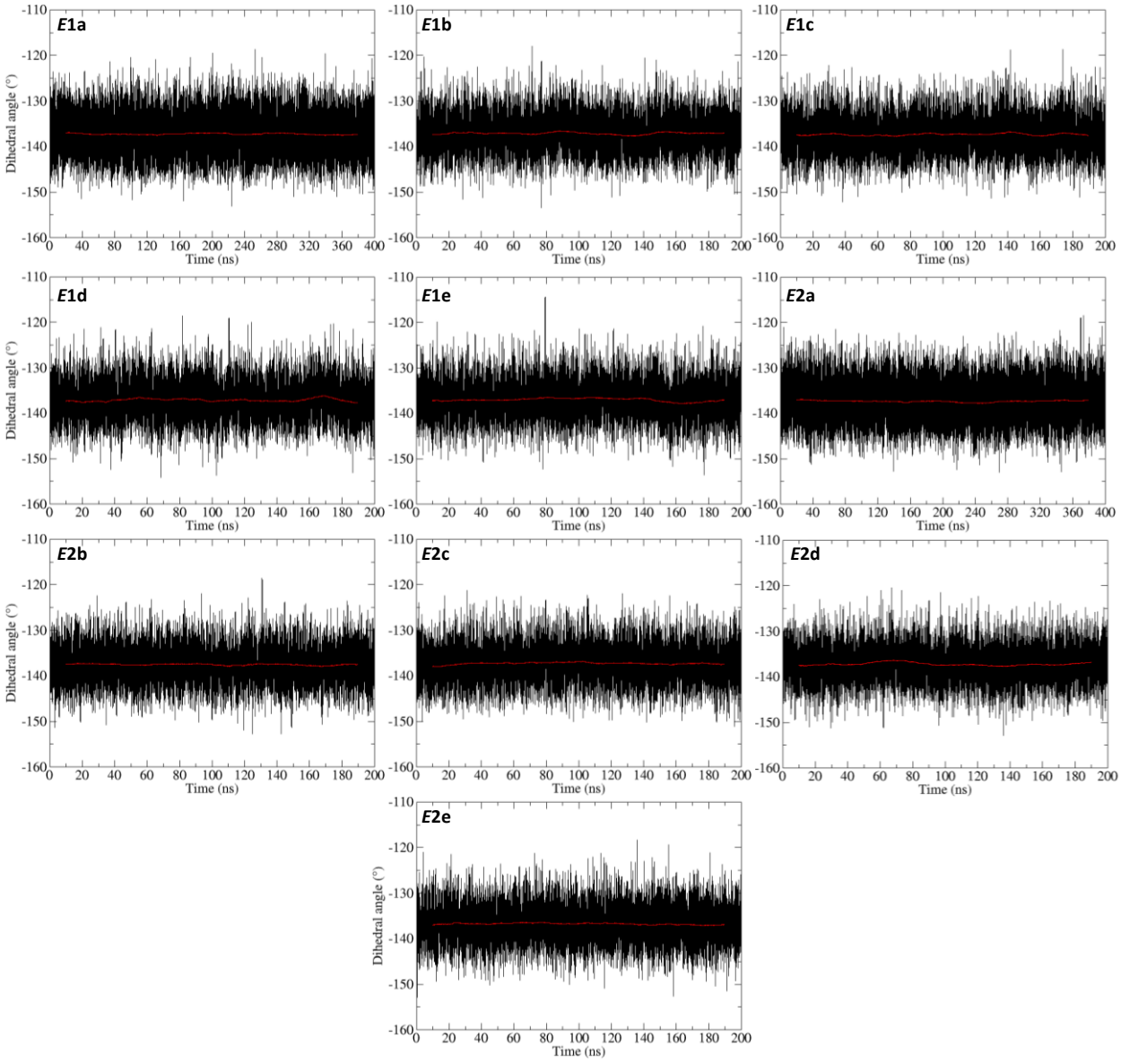

Figure S23. Dihedral angle plot (Time (ns) vs. Dihedral angle (degree)) for *E*-LAB-TEA when placed inside the channel during simulation without K^+-ion. *E*1a to *E*2e represent the starting structure for that particular trajectory. The red line represents the average dihedral angle in degrees.

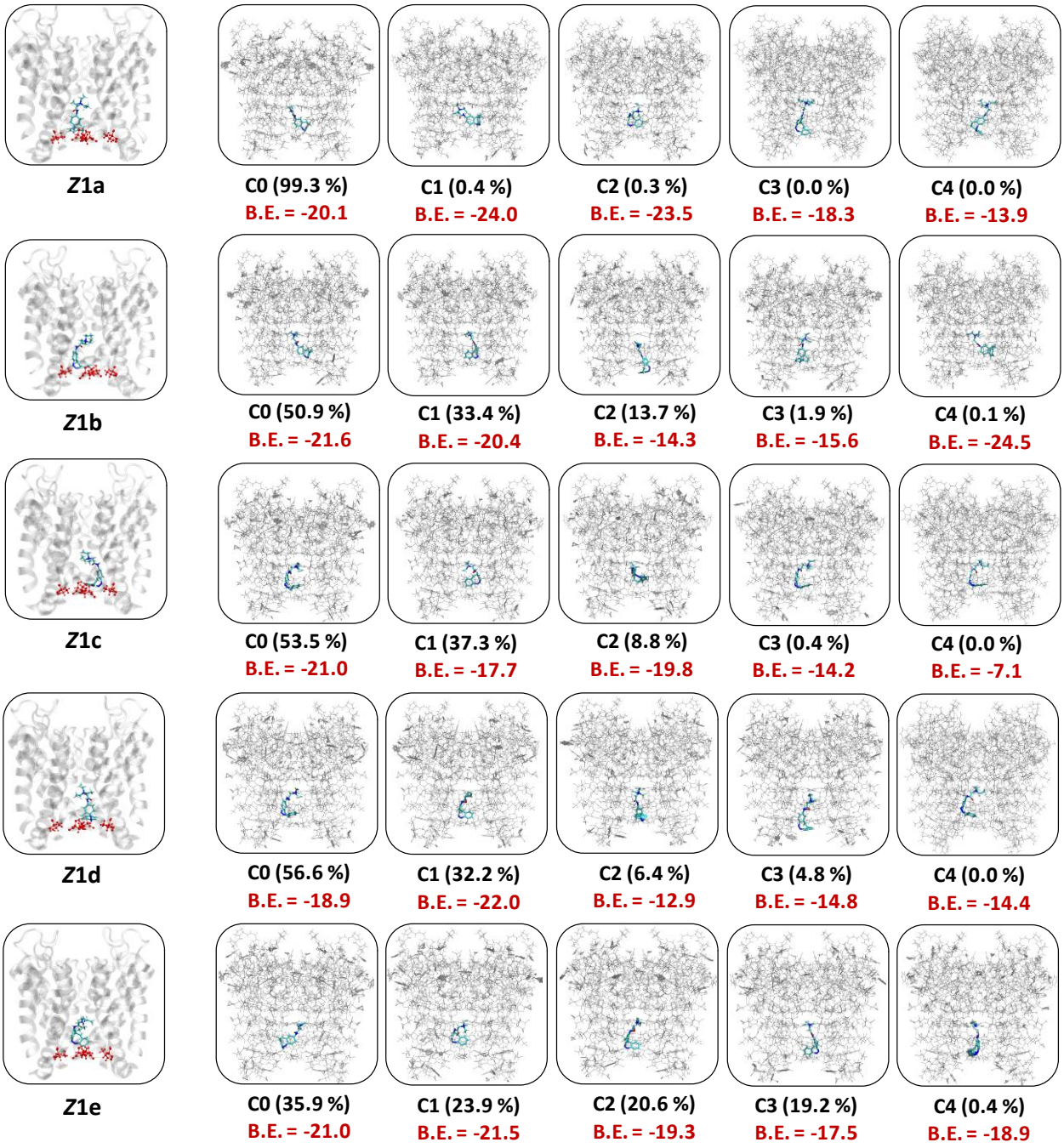

Figure S24. Summary of hierarchical average-linkage clustering performed on trajectories of *Z*-LAB-TEA without K^+-ion, when LAB-TEA placed inside the channel cavity. Z1a to *Z*1e are the starting structure for that particular trajectory. The average structure of each cluster is shown, indicating location of LAB-TEA relative to the ion channel. Cn (n = 0 − 4) indicates different clusters. Percentage occurrence of each cluster is given in parenthesis. Corresponding binding energy (B.E.) is given in kcal/mol. Protein is represented as new cartoon in the starting structure and as lines in the average structures. LAB-TEA is shown as a stick model. All the simulations retained the Z1 binding poses as that in the starting structure.

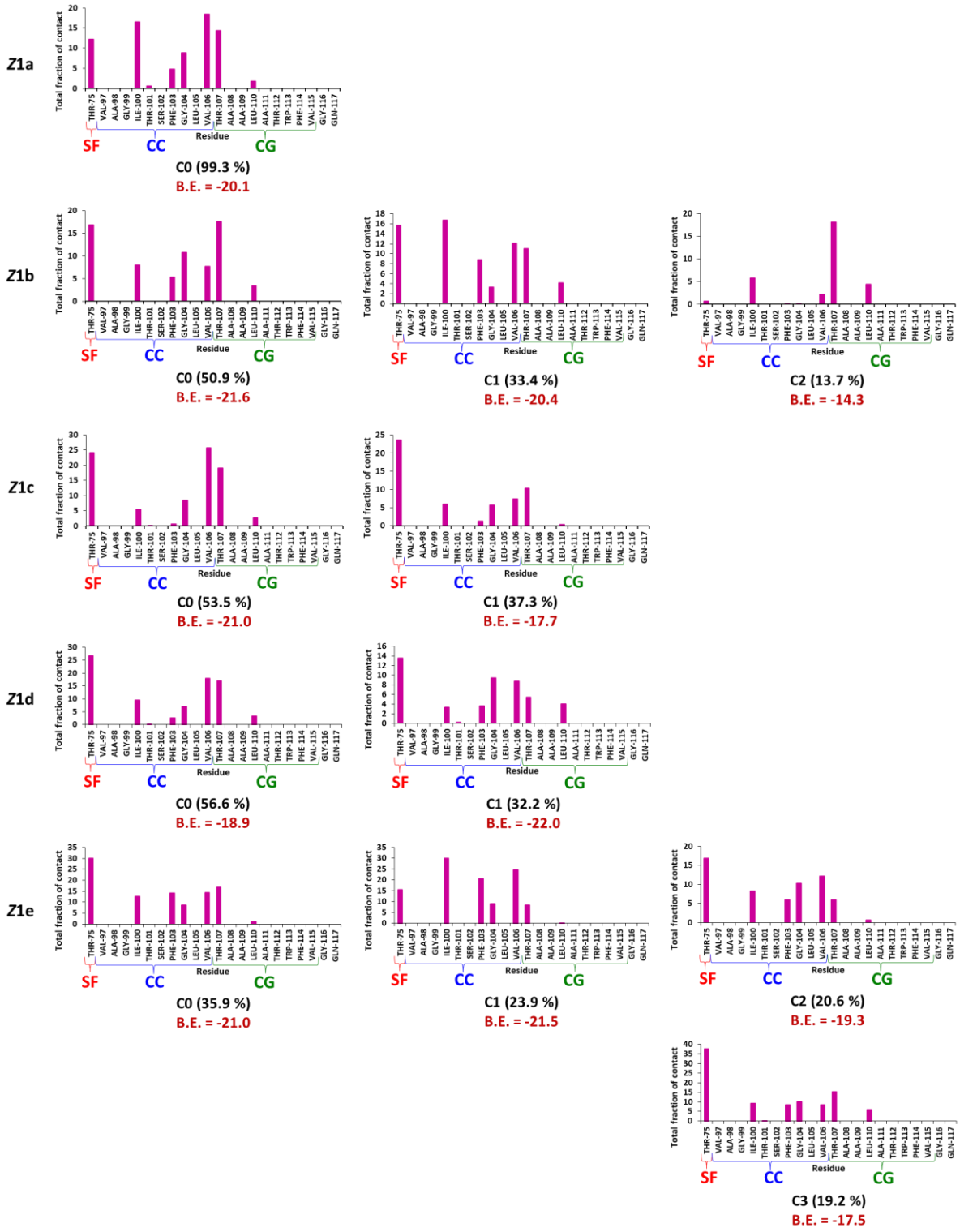

Figure S25. Contact plot per residue for the most probable cluster trajectories (Cn with percentage > 10) of KcsA−Z-LAB-QA without K^+-ion resulting in *Z*1 conformation, when LAB-TEA placed inside the channel cavity. Binding energy in kcal/mol is given in parenthesis. The SF, CC, and CG represent selectivity filter, channel cavity, and channel gate residues respectively.

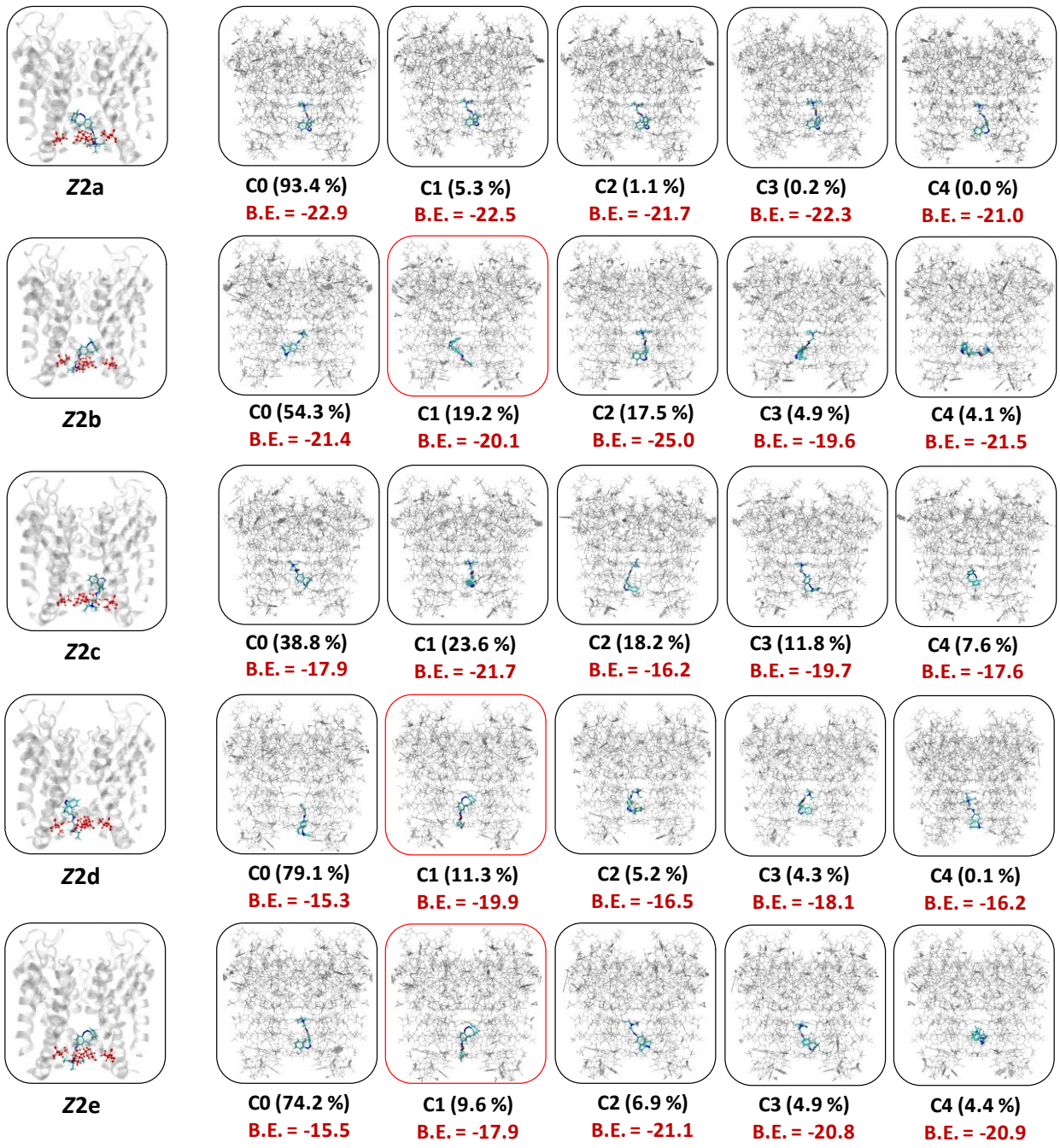

Figure S26. Summary of hierarchical average-linkage clustering performed on trajectories of *Z*-LAB-TEA without K^+-ion, when LAB-TEA placed inside the channel cavity in *Z*2 conformation. *Z*2a to *Z*2e are the starting structure for that particular trajectory. The average structure of each cluster is shown, indicating location of LAB-TEA relative to the ion channel. Cn (n = 0 − 4) indicates different clusters. Percentage occurrence of each cluster is given in parenthesis. Corresponding binding energy (B.E.) is given in kcal/mol. Protein is represented as new cartoon in the starting structure and as lines in the average structures. LAB-TEA is shown as a stick model. All the simulations result in *Z*2 to *Z*1 conversion. The clusters showing *Z*2 conformation is highlighted in red (9.6 - 11.3%).

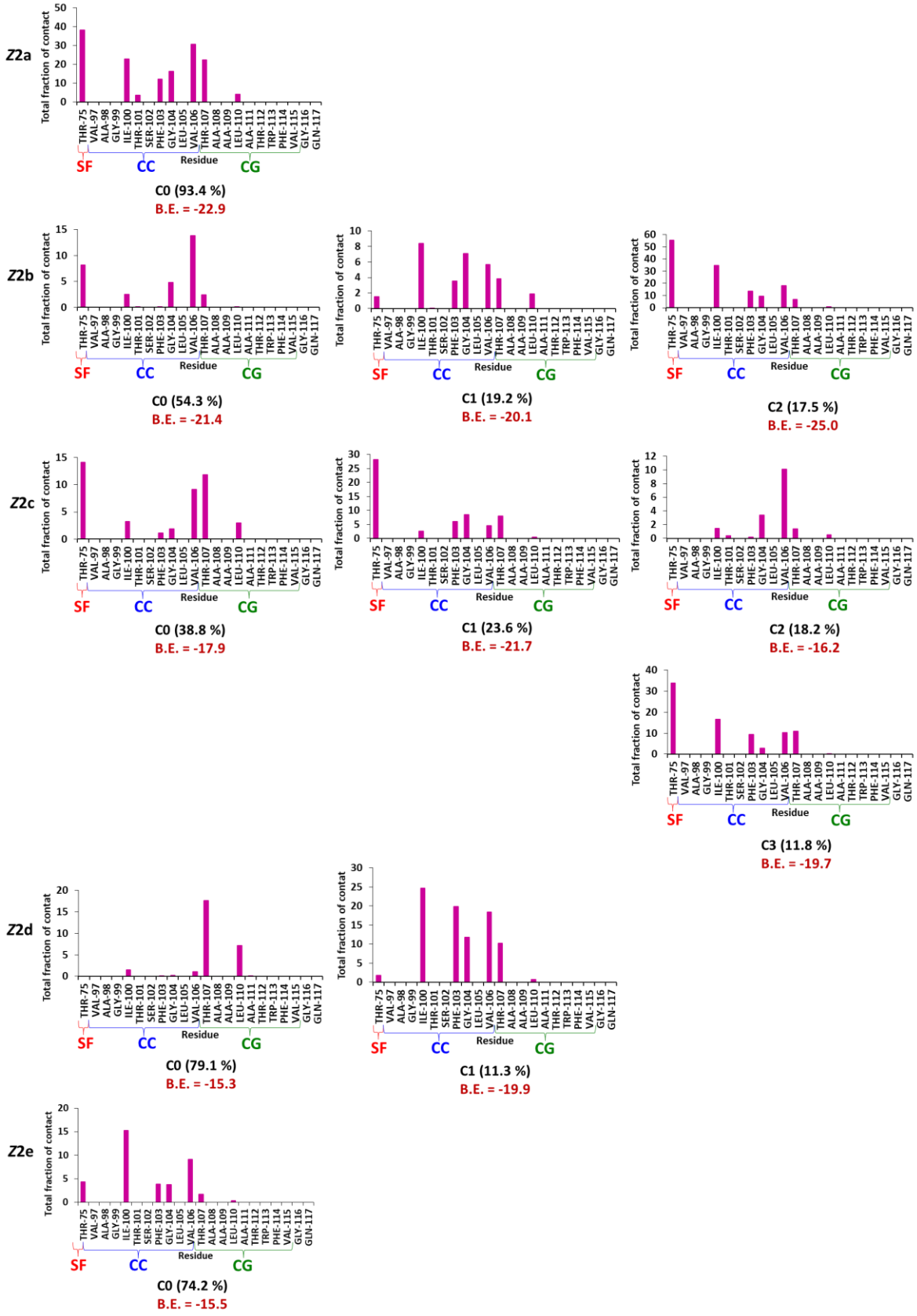

Figure S27. Contact plot per residue for the most probable cluster trajectories (Cn with percentage

> 10) of KcsA−*Z*-LAB-TEA without K^+-ion resulting in *Z*1 and *Z*2 conformations, when LAB-TEA placed inside the channel cavity in *Z*2 conformation. Binding energy in kcal/mol is given in parenthesis. The SF, CC, and CG represent selectivity filter, channel cavity, and channel gate residues respectively.

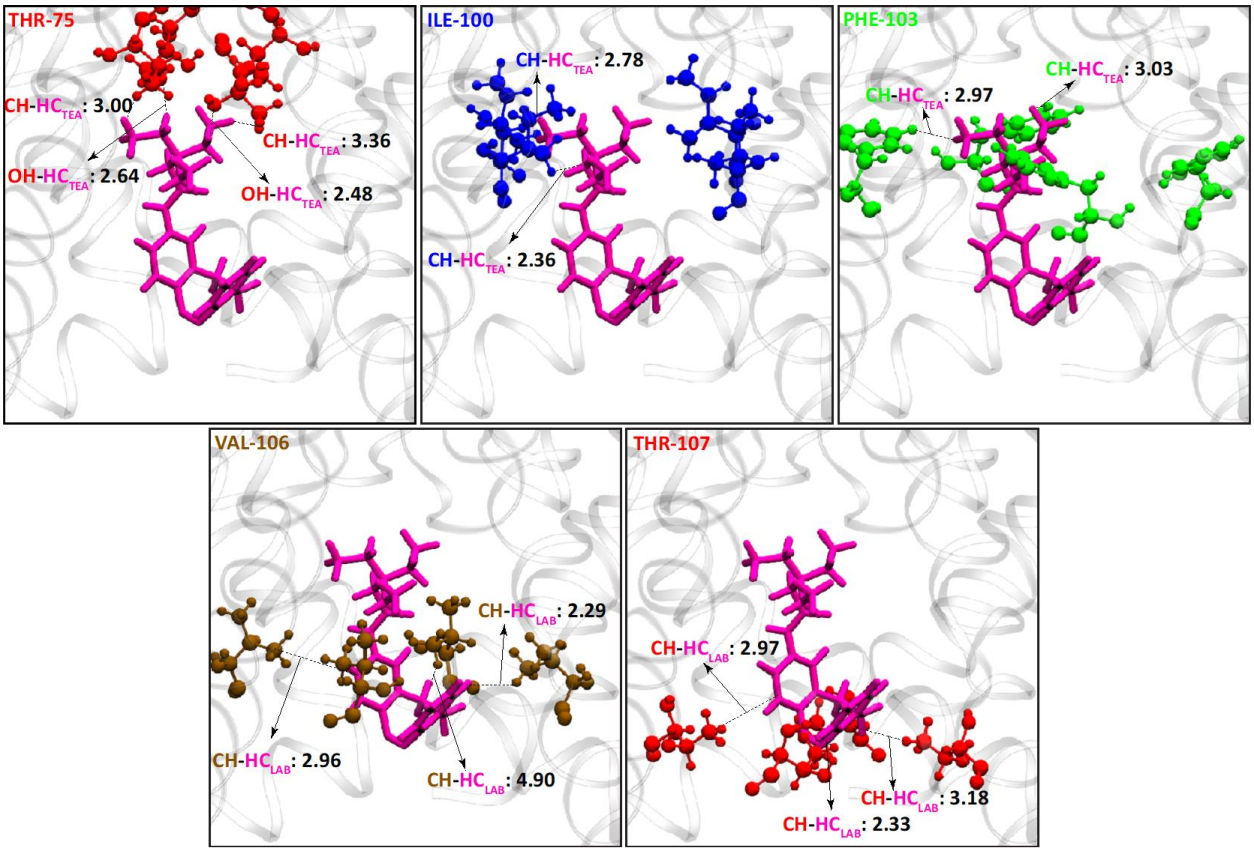

Figure S28. Interaction of *Z*1 conformation with individual channel residues in the most probable conformation (C0), of the trajectory resulting in *Z*1, when simulation performed with *Z*-LAB-QA inside the channel cavity, without K^+-ion. The protein and *Z*1 represented as ribbon and stick (magenta) respectively, and the interacting residues THR-75 (red), ILE-100 (blue), PHE-103 (green), VAL-106 (ochre), and THR-107 (red) from extracellular to intracellular region in ball and stick model. The distances are given in Angstrom. Residue numbers are given in the upper left corner of each box.

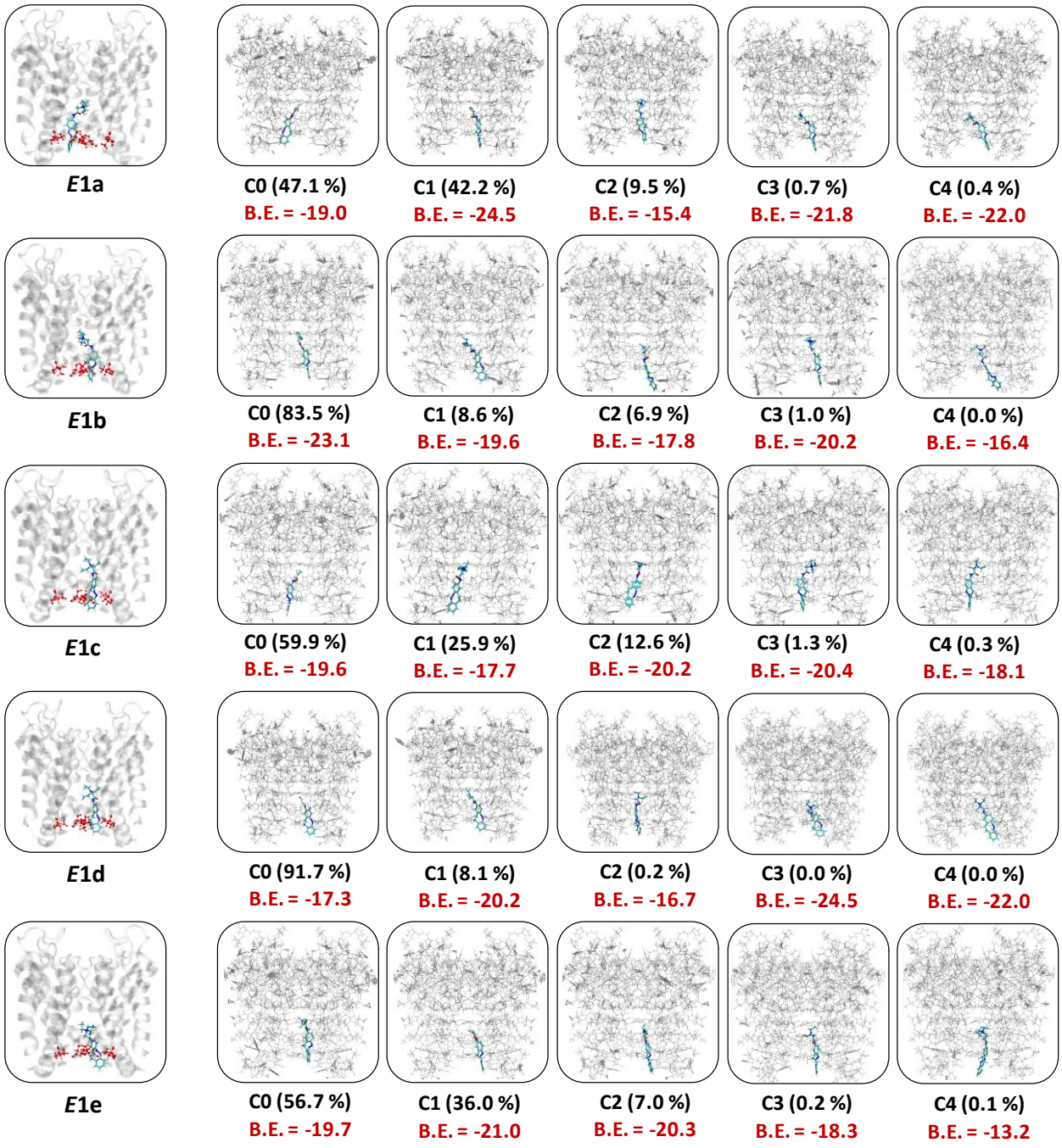

Figure S29. Summary of hierarchical average-linkage clustering performed on trajectories of *E*-LAB-TEA without K^+-ion, when LAB-TEA placed inside the channel cavity. *E*a to *E*c are the starting structure for that particular trajectory. The average structure of each cluster is shown, indicating location of LAB-TEA relative to the ion channel. Cn (n = 0 − 4) indicates different clusters. Percentage occurrence of each cluster is given in parenthesis. Corresponding binding energy (B.E.) is given in kcal/mol. Protein is represented as new cartoon in the starting structure and as lines in the average structures. LAB-TEA is shown as a stick model. All the simulations retained the *E*1 binding poses as that in the starting structure.

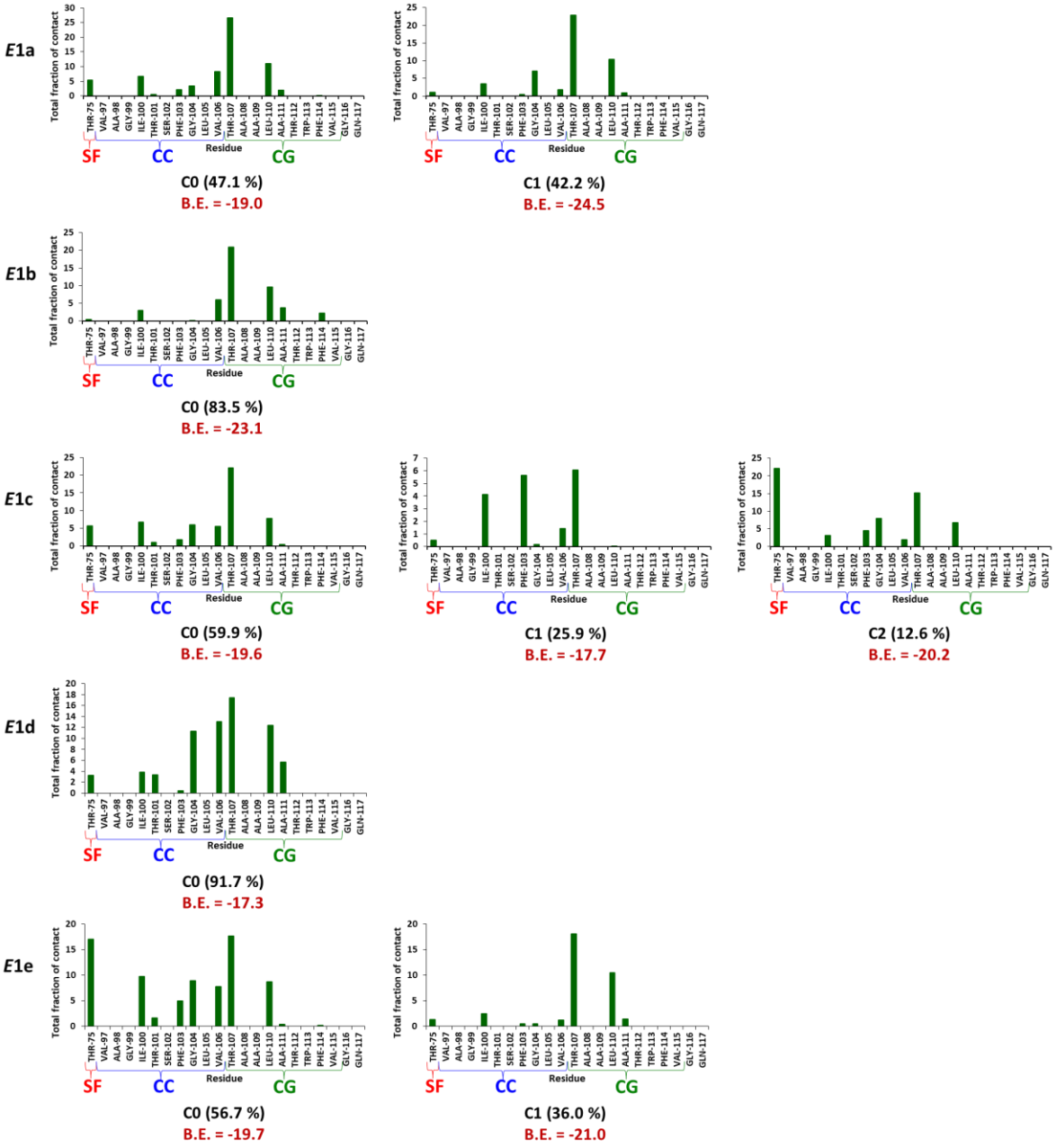

Figure S30. Contact plot per residue for the most probable cluster trajectories (Cn with percentage > 10) of KcsA−*E*-LAB-TEA without K^+-ion resulting in *E*1 conformation, when LAB-TEA placed inside the channel cavity in *E*1 conformation. Binding energy in kcal/mol is given in parenthesis. The SF, CC, and CG represent selectivity filter, channel cavity, and channel gate residues respectively.

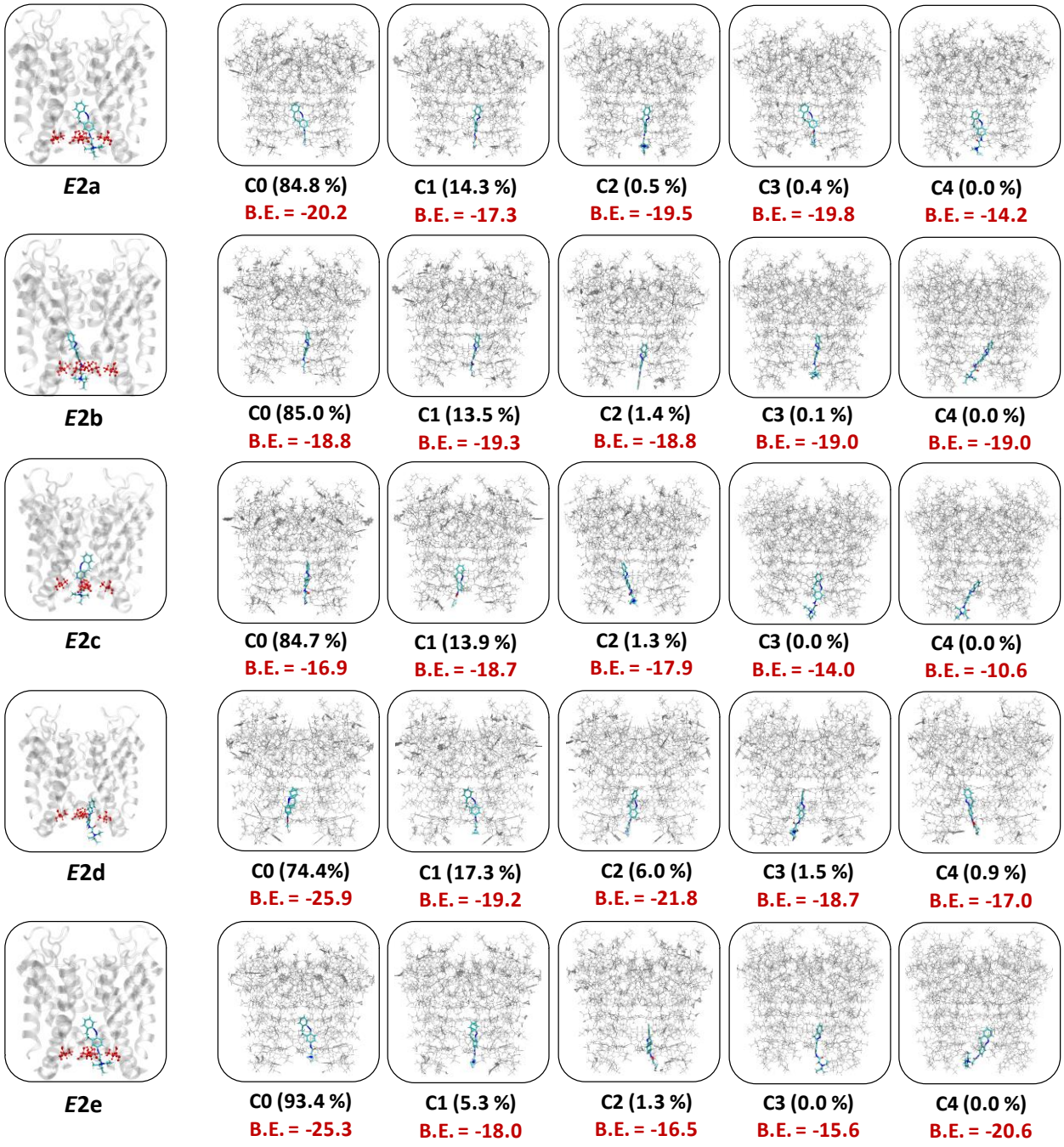

Figure S31. Summary of hierarchical average-linkage clustering performed on trajectories of *E*-LAB-TEA without K^+-ion, when LAB-TEA placed inside the channel cavity. *E*2a to *E*2e are the starting structure for that particular trajectory. The average structure of each cluster is shown, indicating location of LAB-TEA relative to the ion channel. Cn (n = 0–4) indicates different clusters. Percentage occurrence of each cluster is given in parenthesis. Corresponding binding energy (B.E.) is given in kcal/mol. Protein is represented as new cartoon in the starting structure and as lines in the average structures. LAB-TEA is shown as a stick model. All the simulations retained the *E*2 binding poses as that in the starting structure.

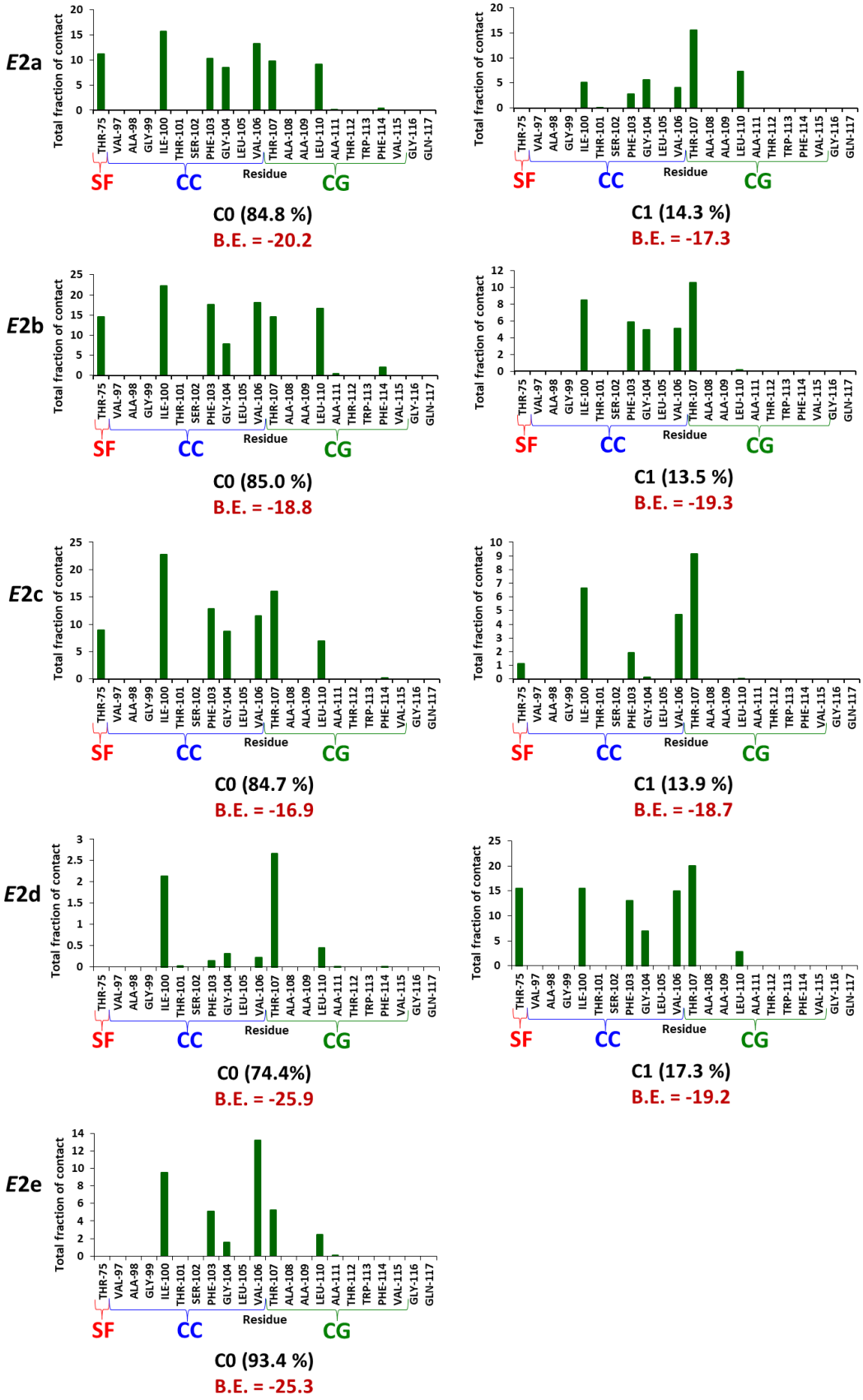
E2a
Total fraction of contact
THR-75 VAL-97 ALA-98 GLY-99 ILE-100 THR-101 SER-102 PHE-103 GLY-104 LEU-105 VAL-106 THR-107 ALA-108 ALA-109 LEU-110 ALA-111 THR-112 TRP-113 PHE-114 VAL-115 GLY-116 GLN-117
Residue
SF
CC
CG
C0 (84.8 %)
B.E. = -20.2
C1 (14.3 %)
B.E. = -17.3
E2b
C0 (85.0 %)
B.E. = -18.8
C1 (13.5 %)
B.E. = -19.3
E2c
C0 (84.7 %)
B.E. = -16.9
C1 (13.9 %)
B.E. = -18.7
E2d
C0 (74.4%)
B.E. = -25.9
C1 (17.3 %)
B.E. = -19.2
E2e
C0 (93.4 %)
B.E. = -25.3

Figure S32. Contact plot per residue for the most probable cluster trajectories (Cn with percentage > 10) of KcsA−*E*-LAB-TEA without K^+-ion resulting in *E*2 conformation, when LAB-TEA placed inside the channel cavity in *E*2 conformation. Binding energy in kcal/mol is given in parenthesis. The SF, CC, and CG represent selectivity filter, channel cavity, and channel gate residues respectively.

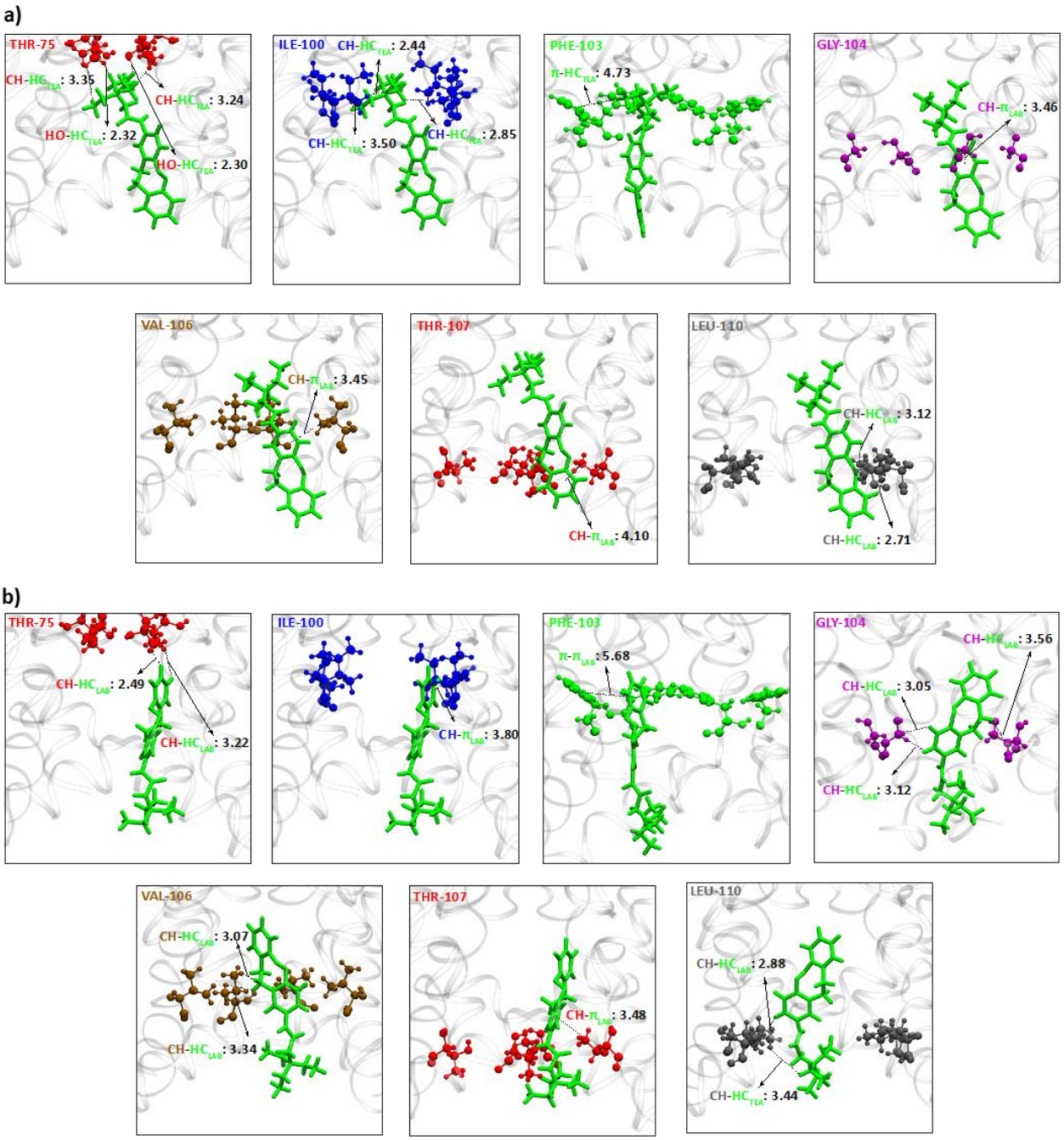

Figure S33. Interaction of (a) *E*1 and (b) *E*2 conformation with individual channel residues in the most probable conformation (C0), when simulation performed with *E*-LAB-TEA inside the channel cavity, without K^+-ion. The protein and *E*-LAB-TEA are represented as ribbon and stick (green) respectively, and the interacting residues THR-75 (red), ILE-100 (blue), PHE-103 (green),

GLY- 104 (purple), VAL-106 (ochre), THR-107 (red), and LEU-110 (grey) from extracellular to the intracellular region in the ball and stick model. The distances are given in Angstrom. Residue numbers are given in the upper left corner of each box.

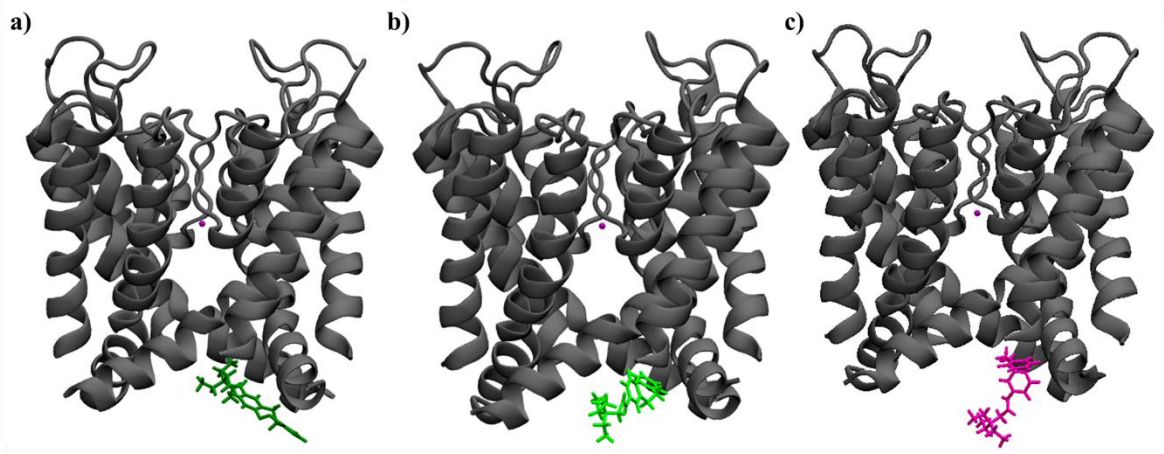

Figure S34. The structure of a) *E*1, b) *E*2, and c) *Z*1 corresponds to the first energy barrier in Figure 10, where *E*1(dark green), *E*2 (green), and *Z*1 (magenta) encounter the channel gate residues for the first time during their transition from the intracellular region. The KcsA channel is shown in ribbon and K^+-ion is shown as the purple ball.

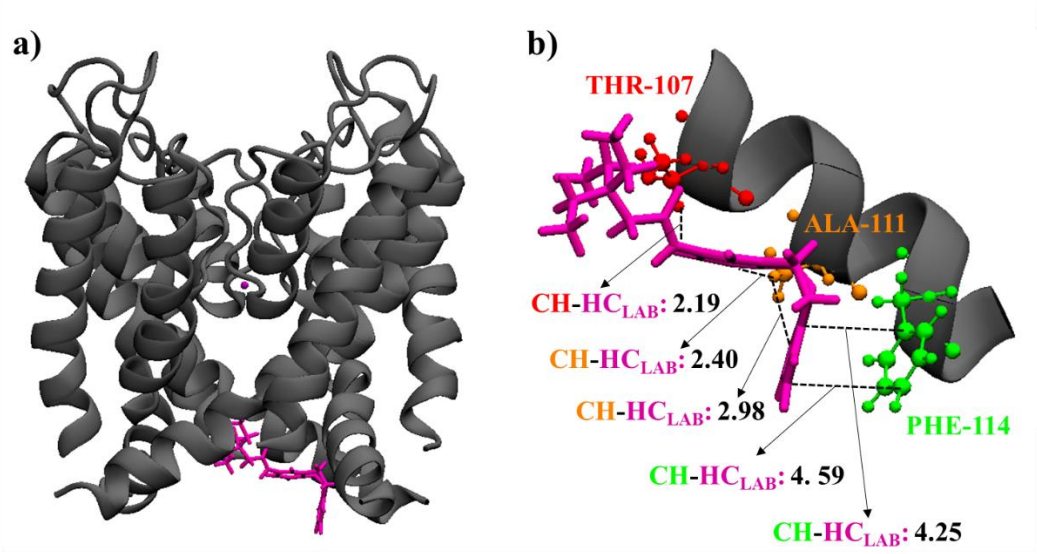

Figure S35. The structure of a) *Z*1 corresponds to the energy 'dip' in the PMF plot, Figure 10. b) Possible interactions of LAB moiety of *Z*1 with the channel gate residues. The KcsA channel is shown in ribbon and K^+-ion is shown as the purple ball.

Supplementary Table S1

Table S1. The calculated binding energy (ΔH) and entropy contribution (TΔS) using the molecular mechanics Poisson Boltzmann surface area (MMPBSA) and the Kongsted Ryde entropy methods respectively are given.

Starting structure	Cluster (% Population)	Conformation	ΔH	TΔS	ΔH-TΔS
			in kcal/mol		
*Z*1a	C0 (71.6)	*Z*1	-21.6	-22.1	0.5
*Z*1h	C0 (32.3)	*Z*2	-17.0	-20.3	3.3
*E*1a	C0 (81.4)	*E*1	-19.2	-20.3	1.1
	C1 (10.2)	*E*1	-16.6	-23.2	6.6
*E*1b	C0 (87.2)	*E*1	-22.3	-20.9	-1.4
*E*1d	C0 (41.7)	*E*1	-20.6	-21.6	1.0
	C1 (38.1)	*E*1	-20.4	-19.7	-0.7
*E*1f	C0 (95.5)	*E*1	-18.9	-20.2	1.4
*E*1g	C0 (46.9)	*E*1	-18.9	-19.9	1.1
	C1 (36.8)	*E*1	-19.7	-20.8	1.1
*E*1h	C0 (84.3)	*E*1	-21.4	-20.6	-0.8
*E*2b	C1 (23.5)	*E*2	-19.0	-19.5	0.5
	C2 (22.1)	*E*2	-15.1	-19.4	4.3
*E*2d	C0 (64.9)	*E*2	-19.0	-18.3	-0.7
*E*2e	C0 (90.9)	*E*2	-18.5	-19.8	1.4
*E*2g	C0 (67.4)	*E*2	-15.3	-25.2	10.0
*E*2h	C0 (93.4)	*E*2	-19.8	-19.2	-0.6
*E*1c	C1 (39.8)	*E*2	-18.6	-20.0	1.4
*E*1e	C0 (87.6)	*E*2	-18.1	-17.5	-0.6

LAB-TEA binding accompanies high entropy contribution, as a free ligand bind inside the channel cavity.